# Quench Probe and Quench Factor Analysis of Aluminum Alloys in Distilled Water

by

Marco Fontecchio

A Master's Thesis

Submitted to the Faculty

of

WORCESTER POLYTECHNIC INSTITUTE

*in partial fulfillment of the requirements for the*

Degree of Master of Science

in

Materials Science and Engineering

by

_____

May 2002

APPROVED:

_____

Richard D. Sisson Jr., Advisor
Professor of Mechanical Engineering
Materials Science and Engineering Program Head

## ABSTRACT

A 6061 aluminum probe was quenched with a CHTE probe-quenching system in distilled water while varying bath temperature and the level of agitation. Time vs. temperature data was collected during the quench by use of an ungrounded K-type thermocouple embedded inside the probe. Cooling rates and heat transfer coefficients, h, were calculated and Quench Factor Analysis (QFA) was also performed to quantitatively classify the quench severity. The data showed an increase in both maximum cooling rate and heat transfer coefficient and a decrease in the Quench Factor, Q, as bath temperature decreased and agitation level increased. Maximum heat transfer coefficient values ranged from 1000 $W/m^2K$ to 3900 $W/m^2K$ while maximum cooling rates of 50°C/s to 190°C/s were achieved. In addition, it was found that at higher levels of agitation, there was also an increase in the standard deviation of the cooling rate.

## ACKNOWLEDGEMENTS

This project could not have been completed without the guidance and direction from my advisor, Professor R.D. Sisson Jr. who aided from start to finish with advice on everything from test procedure to data analysis. He was also gave significant help in troubleshooting the test set-up. In addition, the constant hands-on help from Dr. Md. Manirumizzan was instrumental in facilitating the completion of the experimental testing and design of experimentation. And finally, I would like to thank Todd Billings, Steve Derosier, and Jim Johnston for their constant help in preparing my metallurgical test pieces.

This project was funded by the Center for Heat Treating Excellence (CHTE) and could not have been completed without its financial assistance and desire for quenching data. In addition, I would like to thank the committee that selected me as the recipient of the Stoddard Fellowship for they made it financially possible for me to attend graduate school this past year.

Without the help of the aforementioned people above, this research could not have been conducted and finished in a timely manner. For these reasons, a sincere thank you goes out to all of them.

May 29, 2002

Marco Fontecchio

# LIST OF TABLES

# LIST OF FIGURES

# TABLE OF CONTENTS

# 1.0 INTRODUCTION

Solution heat-treating of aluminum alloys allows the maximum concentration of a hardening solute to be dissolved into solution. This procedure is typically carried out by heating the alloy to a temperature at which one single, solid phase exists [1]. By doing so, the solute atoms that were originally part of a two phase solid solution dissolve into solution and create one single phase. Once the alloy has been heated to the recommended solutionizing temperature, it is quenched at a rapid rate such that the solute atoms do not have enough time to precipitate out of solution [2]. As a result of the quench, a saturated solution now exists between the solute and aluminum matrix.

The cooling rate associated with the quench can be controlled through the variation of the quenching parameters such as bath temperature and degree of agitation. The variation of these parameters allows the heat treater the ability to increase or decrease the cooling rate to achieve certain mechanical properties as well as eliminate distortion and the possibility of cracking [3].

The cooling rate data can be quantitatively characterized by Quench Factor Analysis (QFA). QFA can classify the severity of a particular quench for a particular alloy by one value, Q. Generally speaking, the smaller the quench factor, Q, the higher the quench rate. Totten, Bates, and Mackenzie have done extensive work on the quench factor analysis of aluminum alloys and steel in hopes to prove the validity of QFA and its ability to classify a quench (i.e. the quench conditions and alloy being quenched) [4-9].

## 1.1 Goals and Objectives

The primary goal of this thesis is to experimentally determine the effect that quenching parameters have on the quench severity of 6061 aluminum probes in distilled

water. The parameters of interest include: initial bath temperature and agitation rate. The effects of these parameters will be quantified through the calculation of cooling rates, heat transfer coefficients, and Quench Factor Anaysis..

## 1.2 Thesis Organization

The thesis is divided into six chapters. Chapter 1 is an introduction that provides an overview of the research within and why is it important. Chapter 2 is a thorough review of relevant literature and previous work completed by others in the field of heat treating and quenching. The literature review focuses on the key aspects of the stages of quenching as well as a mathematical analysis called Quench Factor Analysis, which can classify the severity of a quench for the alloy being quenched. These research topics allowed for an understanding of the project at hand. Chapter 3 details the experimental set-up and testing procedures along with a test matrix that laid out the experiments to be conducted. Chapter 3 also describes the equipment used as well as sample preparation and methods for analyzing the collected data. Chapter 4 presents a series of two papers that were written and submitted to journals. The first paper entitled, "The Effect of Temperature and Agitation Level on the Quench Severity of 6061 Aluminum in Distilled Water", written by M. Fontecchio, M. Maniruzzaman, and R.D. Sisson, Jr. describes the effect of quenching parameters through quenching 6061 aluminum in distilled water. This article was submitted to the American Society of Metals' (ASM) 13th Annual International Federation for Heat Treatment & Surface Engineering (IFHTSE) Congress. The second article, entitled, "Quench Factor Analysis and Heat Transfer Coefficient Calculation for 6061 Aluminum Alloy Probed Quenched in Distilled Water", written by M. Fontecchio, M. Maniruzzaman, and R.D. Sisson, Jr. presents a comparison of QFA

and heat transfer coefficients calculations in 6061 aluminum probes. This paper will be submitted to the "Journal of Materials Processing Technology". Chapter 5 is a compilation of conclusions that were drawn, not only in the published papers, but from all research and experimentation conducted in this thesis. The final chapter, Chapter 6, explains how the work could be improved through recommendations on equipment used as well as expanded through the use of polymer quenchants and different alloy types.

# 2.0 LITERATURE REVIEW

The scope of this research covers solution heat treating of aluminum alloys and quenching in distilled water. Factors affecting the effectiveness of the quench, such as, initial bath temperature and degree of agitation were also experimentally determined to fully understand their effect on the overall quench severity [10]. These areas, as well as equations for heat transfer coefficients in a cylinder were calculated in hopes to fully understand the process at hand. Furthermore, a mathematical analysis of quenching, called Quench Factor Analysis, is discussed and illustrates how the severity of a quench can be quantitatively classified for a specific alloy [11].

## 2.1 Solution Heat Treating of Aluminum Alloys

The purpose of solution heat treating in aluminum is to obtain the maximum concentration of the hardening solute, such as zinc, magnesium and copper, in solution by heating the alloy to a temperature in which a single phase will be created [12]. By doing so, the solute atoms that were originally part of a two phase solid solution dissolve back into solution and create one single phase in equilibrium. Once the alloy has been heated for a considerable amount of time, it is quenched at a rapid rate such that the solute atoms do not have enough time to precipitate out of solution. As a result, a saturated solution now exists between the solute and aluminum matrix.

The heat-treating process is best understood by examining a phase diagram to better understand the temperature ranges and phase regions that are involved. These diagrams do not show the actual structures formed during the heat treating processes, but they are a useful tool in predicting the solid-state reactions that will take place at a given temperature and composition [12]. Below, Figure 2.1 illustrates a portion of the

Aluminum–Magnesium phase diagram. The region in which solutionizing can take place for this particular allow lies between 3 and 14.9 wt % Mg, which is the maximum concentration level at which the alloy can be solution heat treated.

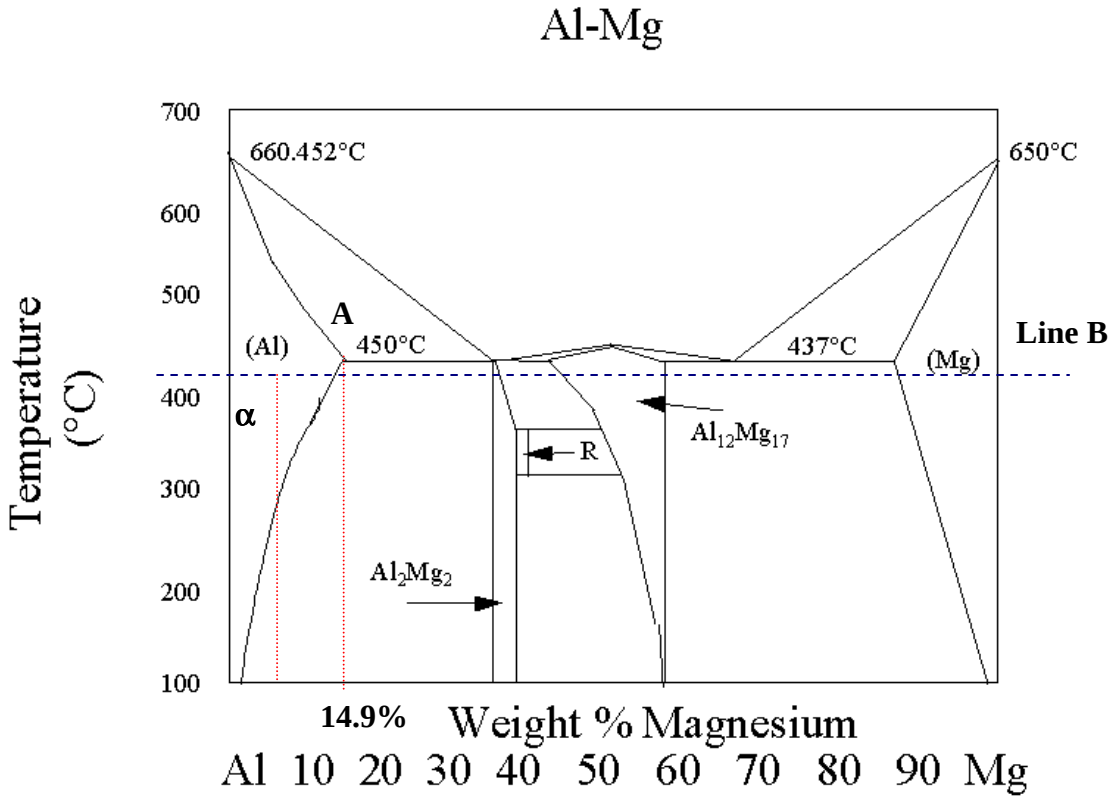


**Figure 2.1:** Aluminum-Magnesium Phase Diagram

**Source:** http://cyberbuzz.gatech.edu/asm_tms/phase_diagrams/pd/al_mg.gif

First, the alloy must be heated into the α range of the diagram. In doing so, the β phase dissolves back into solution and the alloy becomes a homogeneous solution of Al and Mg. The solutionizing temperature is independent upon the concentration of the solute; that is to say, the temperature is the same regardless of the initial amount of Mg in the system [12]. In general, for most commercial applications, the solution heat treating temperature is specified to be 10-15°F below the eutectic temperature (indicated by line

B on the phase diagram); therefore, good control and uniformity of the furnace is essential [2]. Although the temperature range is quite small, more latitude in the solution heat-treating temperature can be tolerated for the 7000 series than for the 2000 series alloys due to the varying amounts of alloying elements [14]. The table below lists the solutionizing temperatures for various solution heat treatable alloys.

| Alloy | Principle Alloying Elements (wt%) | | | | | | | Solutionizing Temperature C |
|---|---|---|---|---|---|---|---|---|
| | Si | Fe | Cu | Mn | Mg | Cr | Zn | |
| 2219 | 0.20 | 0.30 | 5.8 - 6.8 | 0.2 - 0.4 | 0.02 | - | 0.10 | 535 |
| 2024 | 0.50 | 0.50 | 3.8 - 4.9 | 0.3 - 0.9 | 1.2 - 1.8 | 0.10 | 0.25 | 495 |
| 6005 | 0.6 - 0.9 | 0.35 | 0.10 | 0.10 | 0.4 - 0.6 | 0.10 | 0.10 | 530 |
| 6061 | 0.4-0.8 | 0.70 | 0.15 - 0.40 | 0.15 | 0.8 - 1.2 | 0.04 - 0.35 | 0.25 | 530 |
| 6070 | 1.0 - 1.7 | 0.50 | 0.15 - 0.4 | 0.4 - 1.0 | 0.50 - 1.2 | 0.10 | 0.25 | 545 |
| 7075 | 0.40 | 0.50 | 1.2 - 2.0 | 0.30 | 2.1 - 2.9 | 0.18 - 0.28 | 5.1 - 6.1 | 490 |

**Table 2.1:** Solutionizing Temperatures for Various Aluminum Alloys [15]

The time needed for complete solutionizing is not dependent upon the composition of the alloy, but rather the size and shape of the part being heat-treated. In addition, the phase distribution and composition of the alloy plays a large role in the solutionizing time [16]. In general, the time required at the solution heat treatment temperature is dependent upon the product, alloy, fabrication process used, and the section thickness of the material [12]. These factors determine the proportions of the solute that are in and out of solution and the size and distribution of the precipitated phase. For example, sand castings are held at temperature for at least 12 hours, whereas permanent mold castings only require 8 hours of heating due to their finer grain structure [12]. In addition, wrought products heating times are determined from the cross section thickness of the part. Generally, thick slabs are heated for 1 hour per inch of thickness, whereas sheet metal only requires 10-30 minutes. Although the time varies depending on

the size and production method, Table 2.2 illustrates the times needed to heat treat wrought alloys, in general terms [2].

| Thickness (in) | Time (min) | | | |
|---|---|---|---|---|
| | Salt Bath | | Air Furnace | |
| | Min | Max | Min | Max |
| 0.016 and less | 10 | 15 | 20 | 25 |
| 0.017 - 0.020 | 10 | 20 | 20 | 30 |
| 0.021 - 0.032 | 15 | 25 | 25 | 35 |
| 0.033 - 0.063 | 20 | 30 | 30 | 40 |
| 0.064 - 0.090 | 25 | 35 | 35 | 45 |
| 0.091 - 0.125 | 30 | 40 | 40 | 55 |
| 0.126 - 0.250 | 35 | 45 | 55 | 65 |
| 0.251 - 0.500 | 45 | 55 | 65 | 75 |
| 0.501 - 1.00 | 60 | 70 | 90 | 100 |
| Each additional 0.50 inches | Add 20 min | | Add 30 min | |

**Table 2.2**. Soaking Time for Solutionizing of Wrought Aluminum Alloys

In an air furnace, time is measured from when the furnace recovers to the heat treating temperature after the part has been submersed, whereas in a salt bath, time starts at the second the part is immersed (provided it doesn't drop the bath temperature more than 10° F) [17].

## 2.2 Quenching

Once the material has been held at temperature for a sufficient amount of time, it is then rapidly quenched to room temperature to preserve the solute in solution. The cooling rate needs to be fast enough to prevent solid-state diffusion and precipitation of the second phase [1]. The rapid quenching creates a saturated solution and allows for increased hardness and improved mechanical properties of the material. In addition, studies have shown that the highest degrees of corrosion resistance have been obtained through the maximum rates of quenching [12].

In general terms, liquid quenching is performed in water, oil, and, more recently, in aqueous polymer solutions. Water and oil quenching cover the extremes in terms of cooling rates, with water being the fastest and oil being the slowest. The introduction of aqueous polymer solutions allowed for cooling rates to be achieved between the two extremes [4].

### 2.2.1 Stages of Quenching

Quenching takes place in three distinct stages, namely: Vapor Blanket Stage, Boiling Stage, and Liquid Cooling Stage. The Vapor Blanket Stage begins when the hot part makes contact with the quenching medium. As the part is submersed, an unbroken vapor blanket surrounds the piece. This blanket exists because the supply of heat from the surface of the part exceeds the amount of heat needed to form the maximum vapor per unit area on the piece [10]. This stage is characterized by a relatively slow cooling rate since the vapor of the quenching medium surrounds the part and acts as an insulator. In this particular stage, heat is removed from the part by radiation and conduction through the vapor layer. As the component cools, the vapor blanket cannot be maintained and therefore breaks down. After this breakdown, the Boiling Stage immediately begins. The surface of the part is now in direct contact with the fluid and results in violent boiling of the medium. This stage is characterized by rapid heat transfer through the heat of vaporization. Size and shape of the vapor bubbles are important in controlling the duration of this stage as well as its corresponding cooling rate [10]. As the part continues to cool below the boiling point of the medium, the Boiling Stage can no longer exist and it too breaks down giving way to the Liquid Cooling Stage. This stage, much like the Vapor Blanket Stage, is also characterized by slow rates of heat transfer. Heat is

dissipated from the part by movement of the quenching medium by conduction currents. The difference in temperature between the boiling point of the medium and actual temperature of the medium is the major factor influencing the rate of heat transfer in liquid quenchants [10]. Furthermore, viscosity of the medium at this point also affects the cooling rate since a less viscous medium will dissipate heat faster than one of high viscosity [18]. The final stage of quenching is the most important in controlling and reducing distortion and cracking [Hasson., 1992 September #24]. Figure 2.2 below illustrates the stages of quenching and where they can be seen on a typical cooling curve as the quench is being monitored. The slope of the curve between the stages is the cooling rate, so it can easily be seen that the first and third stages have slow cooling rates since the slope of the line at those points is small. On the other hand, the slope of the second stage is quite large and therefore, the cooling rate is high.

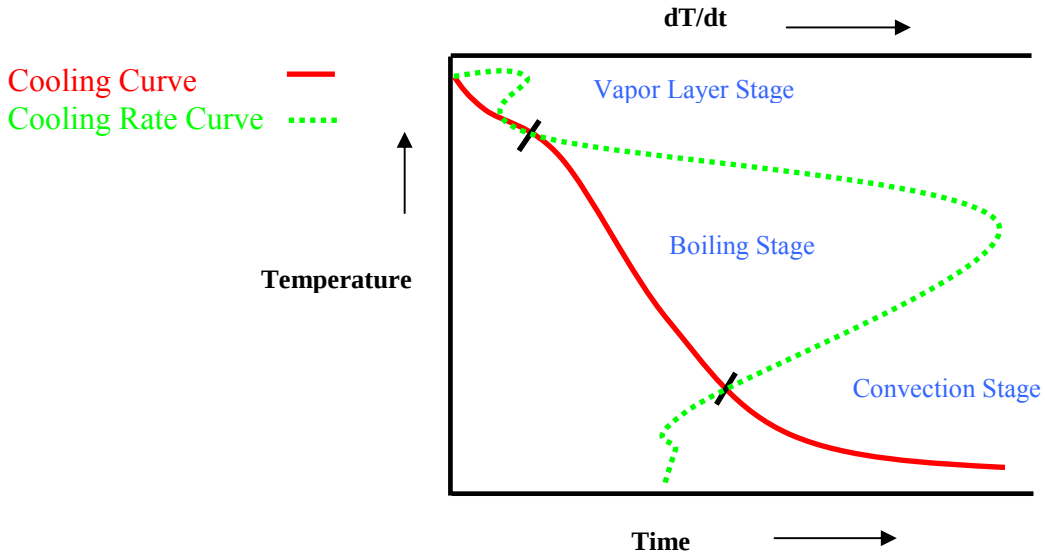


**Figure 2.2:** Typical Cooling Curve with Corresponding Cooling Rate and Stages of Quenching

### 2.2.2 Factors Affecting Quenching

Several factors influence the effectiveness of a quenching medium in its ability to withdraw heat from a quenched part. These factors include: temperature of the medium, degree of agitation, surface conditions of the part, and the type of quenching medium [3]. In addition, the configuration of the quenched part also plays a role in the rate of heat transfer during quenching, but since this particular research mainly deals with simple geometries, it will not be discussed.

#### 2.2.2.1 Effect of Temperature

The temperature of the medium has a drastic effect on its ability to extract heat from a hot part, but that is not to say that the lowering the bath temperature increases the heat transfer rate [8]. The heat extraction is still dependent on the characteristics of the medium itself. In general, higher quenchant temperatures lower the temperature at which a total vapor blanket is maintained in the medium. As a result, it will lengthen the duration of the first stage of quenching, which lengthens the time at which the part is cooled at slower cooling rates [10]. Depending on the medium itself, higher bath temperatures may decrease viscosity, which affects bubble size and therefore, decrease the rate of heat transfer during the third stage of quenching.

In the case of water, since it produces the fastest cooling rates, lower temperatures produce high thermal gradients between the bath and the part [3]. As a result, high thermal stresses will be induced and the risk of distortion or cracking will increase. On the other hand, as the temperature of the water is increased to avoid cracking, the physical properties of the material decrease due to incomplete saturation of the solution during quenching [9].

#### 2.2.2.2 Effect of Agitation

Agitation plays a large role in the effectiveness of a particular medium to quench a part. Some will say that it is the most important factor in determining the success of the quench [9]. In general, agitation increases the rate of heat transfer throughout the quenching process. During the Vapor Blanket Stage, agitations will breakdown the blanket much earlier in the quench and force the Boiling Stage to begin. As a result, a stage of slow cooling is cut short and replaced with a stage of rapid heat transfer. Overall, the part will be cooled at a faster rate. In addition, it will also produce smaller, more frequent bubbles during the Boiling Stage, which, in turn, creates faster rates of heat transfer throughout the part [9].

In terms of its mechanical effects, any solids that have formed on the test piece will be agitated off of the surface and allow for maximum heat transfer since the medium will be in direct contact with the exposed surface. These gels would have acted as an insulating layer to slow down the cooling rate, but with the use of agitation, this layer is mechanically removed and maximum heat transfer can be achieved. Finally, agitation forces cool liquid to constantly be circulated to the workpiece in place of the hot liquid [3]. Therefore, higher temperature differences will always exist between the medium and the surface, resulting in faster rates of heat dissipation [18].

#### 2.2.2.3 Effect of Surface Finish

Lowest cooling rates are observed on surfaced that are newly machined or bright-etched, whereas faster rates are obtained by surfaces with oxide films and stains. In addition, surface roughness has a similar relationship regarding cooling rates; the rougher the surface, the faster the cooling rate [19]. This phenomenon can be attributed to the

stability of the vapor phase on each surface. If the surface is smooth, then the vapor layer becomes uniform and stable, whereas if there are discontinuities on the surface, then it becomes easier to break down the layer and induce the Boiling Stage [9]. Furthermore, the application of non-reflective coatings will increase heating and affect the quench of the material [12]. Figure 2.3 shows the corresponding cooling rate and heating rate for a machined surface and a surface with a black carbon coating (black coated). It is readily seen that the coated surface not only heats up faster, but also is quenched to room temperature faster.

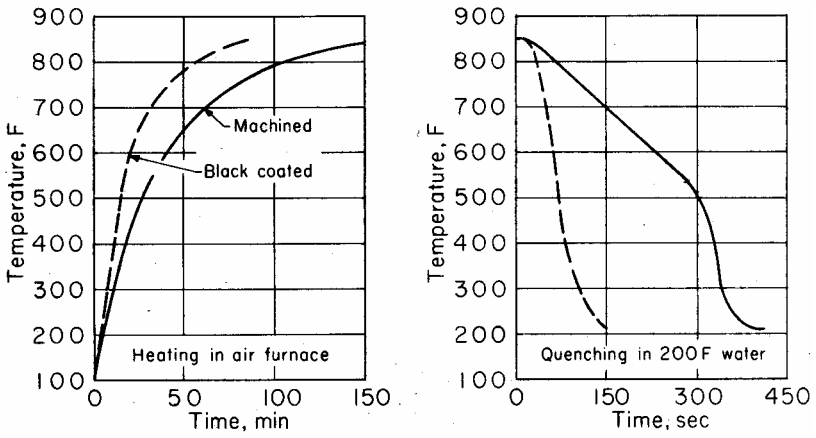


**Source:** [39]

**Figure 2.3:** Effect of Surface Finish on Heating and Cooling of an Aluminum Cylinder

## 2.2.3 Aqueous Quenching Mediums

As mentioned previously, water, oil, and polymer solutions are common quenching mediums for aluminum alloys. The mediums differ in the rate at which they dissipate heat out of a quenched part. Water, by far, has the fastest cooling rate, followed by polymer solutions and finally oil. For the scope of this research, only distilled water will be considered since we are mainly dealing with quenching of aluminum alloys and higher cooling rates are preferred for desirable mechanical properties.

### 2.2.3.1 Water Quenching

Water is widely used in the quenching of non-ferrous alloys, austenitic stainless steels, and many other solution heat treatable alloys. Water is commonly used because it is inexpensive, readily available, and easily disposed of without any health or environmental concerns [12]. It is also one of the fastest quenching mediums and approaches the fastest cooling rate attainable in a liquid bath. As a result, high hardness values can be obtained and excellent mechanical properties can be produced. Although high cooling rates are desirable, they can cause problems in the quenching process. These high cooling rates are consistent throughout the quench, even at low temperatures; therefore, the risk of distortion and cracking is high.

One study showed that water does not sufficiently 'wet' the surface of the aluminum during quenching [20]. There are three distinctly different cooling regimes with dramatically different heat transfer characteristics present on the surface of aluminum during the quench process, which will produce different thermal gradients that will increase distortion [9]. As a result, water is generally used to quench simple geometric parts. If the temperature of the bath is initially low (cold water –> 50-90°F, 10-32°C), a high thermal gradient exists between the part and the quenching medium. If cold water is used and there is a considerable amount of cracking/distortion, an alternative is to increase the bath temperature and quench in hot water (140-160°F, 60-71°C) [9]. As the temperature of the bath increases, there is more of a tendency for the vapor blanket to be prolonged due to the nature of water to form vapor as it approaches the boiling point [Hasson., 1992 September #24]. The obvious disadvantage to this is that the cooling rate will be slower and the desired mechanical properties may not be

achieved. The Boiling and Convection Stage, on the other hand, are not affected by the increase in bath temperature.

Aside from distortion, uneven hardness and soft-spot distribution can be seen with a water quench. The vapor blanket is prolonged, which encourages vapor and bubble entrapment in certain locations. Because of this, uneven heat transfer will be experienced throughout the part and consequently, soft-spots will develop in these areas [12]. Studies have shown that the optimal temperature window for creating uniform quenching and reproducible parts is when the water remains between 15-25°C [17]. Figure 2.4 below illustrates the effect changing the bath temperature has on the stability of the vapor blanket.

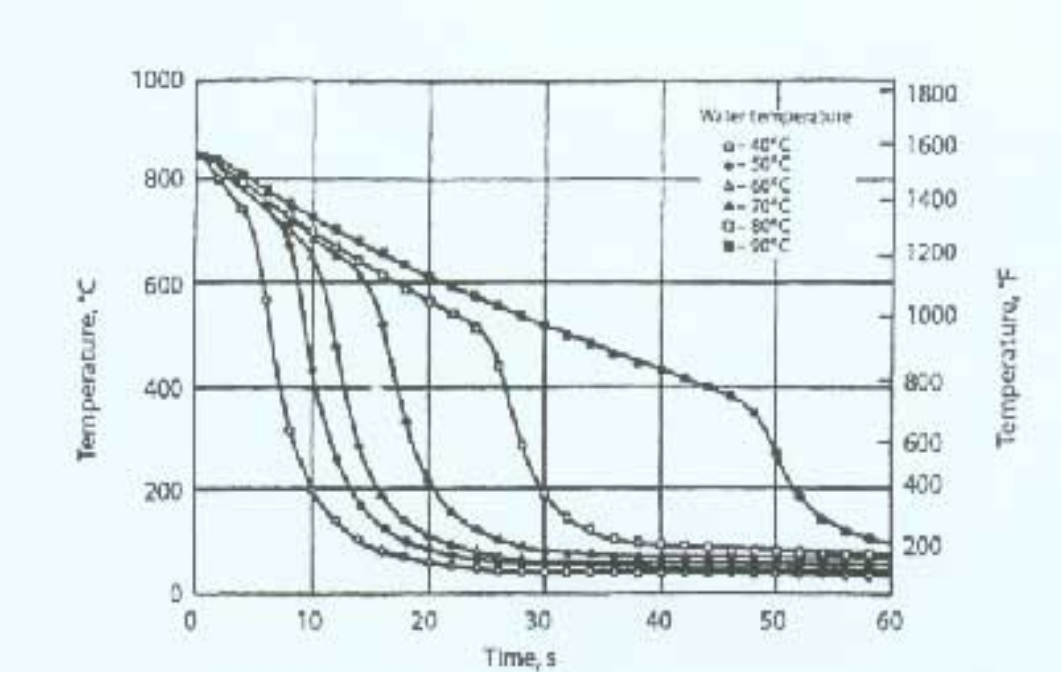


**Figure 2.4:** Effect of Bath Temperature on Quench Rates [10]

As seen above, the cooling rate of the quenched part is increased as the bath temperature is raised from 40 C to 90°C. Furthermore, at temperatures above 50°C, there is an increase in vapor blanket stability as seen by the extended linear region of the

cooling curve. As a result, a stage of low cooling rate is prolonged before giving way to the rapid cooling boiling stage. The study corresponding to the plot above showed that the stability of film boiling is affected by the ability of the agitated fluid to breakdown the vapor blanket [21]. The sensitivity of quench rate as agitation is increased was also correlated to an increase in bath temperature. So, overall, regardless of the bath temperature, the quench rate can still be further varied by the introduction of agitation [21].

## 2.3 Conductive Heat Transfer

Heat transfer deals with the withdrawal of heat or energy from a body. There are three methods of heat transfer, namely: conduction, convection and radiation [18]. For the scope of this analysis, conduction and convection are discussed while radiation does not play an important role. The best way for fully understand conduction is to analyze a differential element of size $\Delta x$ of constant mass equal to the density times volume ($\rho V$). This derivation will allow complete understanding of the origin of the useful equations and theories. The figure below depicts a differential element with heat entering and leaving.

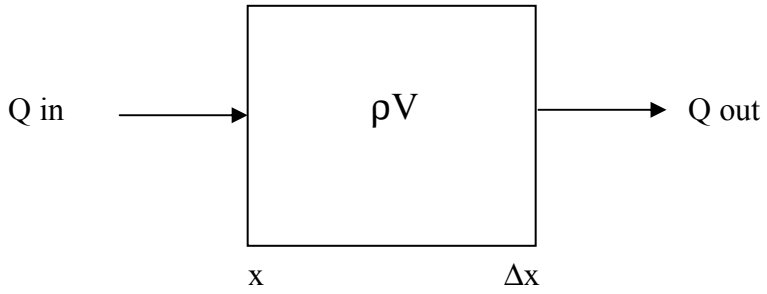


**Figure 2.5:** Differential Element of Size $\Delta x$

Above illustrates an open system where heat is entering and leaving. It is also important to note that no heat is being generated within the body. So, by the first law of thermodynamics, the conservation of energy states that the change in internal energy of the system is equal to the heat transferred into the system minus the heat generated within the system [18]. In mathematical representation:

$$\frac{dU}{dt} = Q_{transferred} + Q_{Generated} \quad \textbf{(2.1)}$$

As illustrated above, the system has a fixed mass of ρV, so we can substitute dU = ρVdu, where u is the specific internal energy of the body. In addition, for an incompressible solid, du = $c_v$dT, where $c_v$ is the constant volume specific heat. The heat transfer is also taking place through a constant cross-section 'A". Now, we can substitute into the above equation and get the following:

$$\rho V c_p A \frac{dT}{dt} = Q_{transferred} + Q_{generated} \quad \textbf{(2.2)}$$

The left side of the equation is finished, but the right side must be simplified. We know that no generation is taking place, so $Q_{generated}$ = 0 and $Q_{transferred}$ can be determined by a simple heat balance from Figure 2.5.

$$Q_{transferred} = Q_{out} - Q_{in} = \frac{-A[Q(x+\Delta x) - Q(x)]}{dx} \quad \textbf{(2.3)}$$

By simplifying the right side, we get the following:

$$Q_{transferred} = Q_{out} - Q_{in} = -A\frac{dQ}{dx} \quad \textbf{(2.4)}$$

As a result of the above simplifications and substitutions, we can rewrite the general equation. It can be seen below.

$$\rho V c_p A \frac{dT}{dt} = -A\frac{dQ}{dx} \quad \textbf{(2.5)}$$

The area (A) will cancel out and Q can be substituted with Q = -k dT/dx. This relationship is known as Fourier's Law for Conduction. Finally, the general equation can be written as:

$$\frac{1}{K}\frac{dT}{dt} = \frac{d^2T}{dx^2} \qquad Where\ \frac{1}{K} = \frac{\rho V c_p}{k} \quad \textbf{2.(6)}$$

ρ = Material Density [kg/m$^3$]
$c_p$= Specific Heat [J/kg K]
V = Volume of Part [m$^3$]
k = Thermal Conductivity [W/m K]
T = Absolute Temperatuer [K]

This final equation is Fourier's Second Law for heat conduction in a solid [18].

### 2.3.1 Physical Properties of 6061 Aluminum

The physical properties of 6061 aluminum are not constant over all temperature ranges[22, 23]. That is to say, as the temperature increases or decreases, the properties will change. For the purpose of this research, values of the specific heat, $c_p$, density, ρ, and thermal conductivity, k, of 6061 aluminum will be utilized for calculations of heat transfer coefficients and the Biot number. The values used for these physical variables

will be calculated as a function of temperature during the quench in order to increase the accuracy of the calculations. Below, Figure 2.7 shows the dependency of $c_p$ on temperature for various aluminum alloys [22].

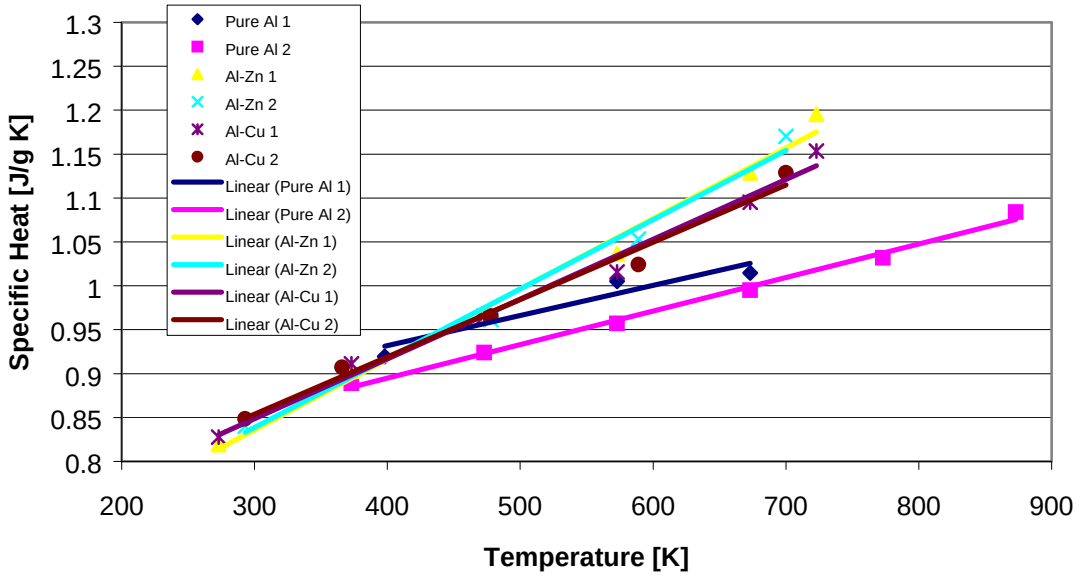


**Figure 2.6:** Specific Heat as a Function of Temperature for Various Aluminum Alloys

It can be seen that the lines of best fit for the four alloys all lie directly on each other whereas the curves for pure aluminum deviate from them at higher temperatures. For this reason, it will be assumed that the specific heat of 6061 aluminum will follow a similar trend as the other alloys presented within the figure. In addition, the specific heat of 6061 aluminum at room temperature is equal to 0.896 J/g K, which falls directly on the line of best fit above. For these reasons, it will be assumed that 6061 will follow similar trends at higher temperatures and the curve with equation equal to Cp [J/KgK] = 0.007T + 0.644, will be used for our heat transfer coefficient calculations.

In addition, the density, ρ, of the material can be calculated as a function of temperature. The density of the material is not constant because the volume of the part will increase with increasing temperature.

$$\rho = \frac{m}{(l_o + l_o \alpha \Delta T)(d_o + d_o \alpha \Delta T)^2} \quad \textbf{(2.7)}$$

m = mass of probe [g]
α = Coefficient of thermal expansion [cm/cmK]
$l_o$ = Initial length of probe at room temp [cm]
$d_o$ = Initial diameter of probe at room temp [cm]
ΔT = Change in temperature ($T_{part}$ - 273) [K]

The coefficient of thermal expansion, α, for 6061 aluminum is equal to 2.26 x $10^{-6}$ /K[2]. The equation below illustrates the formula used to calculate the density as a function of temperature.

The plot below shows the dependence of density on temperature. It is clear to see that the relationship of density to temperature is linear, but with an extremely small, negative slope. So, the variation in density over the temperature range of interest is quite small. The values range from 1.875g/$cm^3$ to 1.94 g/$cm^3$, which is a variation of only 1.7% about the mean. For this reason, it will be assumed that the density is constant and a value equal to 1.905 g/$cm^3$ will be used in our calculations.

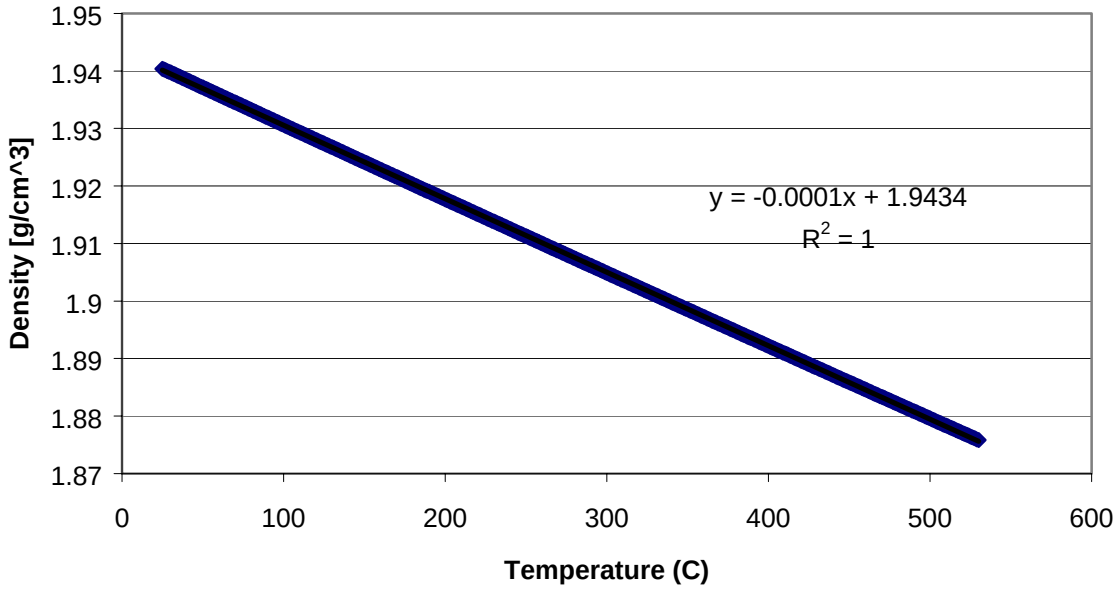


**Figure 2.7:** Density Variation of 6061 Aluminum as a Function of Temperature

Finally, Figure 2.8, below, shows the dependency of the thermal conductivity, k, for an Aluminum-Magnesium Alloy as a function of temperature [23].

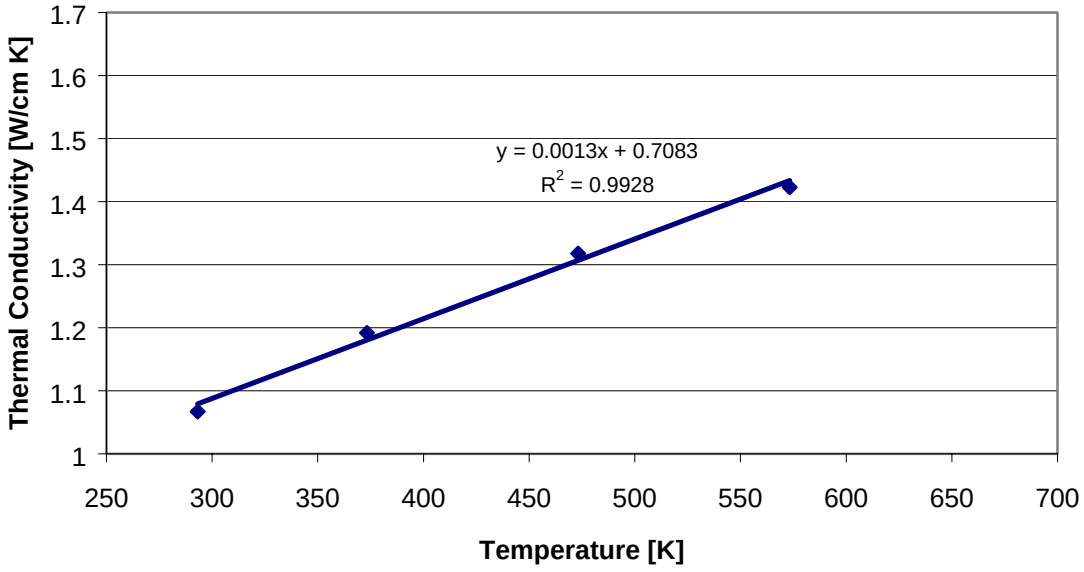


**Figure 2.8:** Thermal Conductivity of an Aluminum-Magnesium Alloy as a Function of Temperature

This particular plot is not data directly taken from alloy 6061, but the chemical composition is very similar and will be used for the Biot Number calculation

### 2.3.2 Heat Transfer Coefficient *h*

The heat transfer coefficient '*h*' [W/ $m^2$ K] during quenching can be calculated by an inverse method. This procedure is done by calculating the cooling rate (dT/dt) that is taking place in the part, and then using it to calculate the heat transfer coefficient h. Since time and temperature curves are continually collected via data acquisition software, it is a simple derivative of the curve that allows us to calculate the cooling rate.

The following equation was derived and will be used in relevant calculations of the heat transfer coefficient.

$$\rho V c_p \frac{dT}{dt} = -hA(T_s - T_l) \qquad \textbf{(2.8)}$$

The above equation can be manipulated to directly solve for h. The equation is shown below:

$$h = \frac{\rho V c_p \frac{dT}{dt}}{A(T_s - T_l)} \qquad \textbf{(2.9)}$$

$T_s$ = temperature of the part [K]
$T_l$ = temperature of the quenching liquid [K]
A = surface area of the part being quenched [$m^2$]
V = volume of part [$m^3$]

The above equation is derived from convective properties of the medium with respect to the quenched body [19].

### 2.3.3The Biot Number

The Biot number can be defined as the ratio of internal conduction resistance to external convective resistance. The mathematical equation of the Biot number is shown below.

$$Bi = \frac{hL}{k} \tag{2.10}$$

h = heat transfer coefficient [W/m$^2$K]
L = characteristic length for the part [r/2] [m]
k = thermal conductivity of the quenched part [W/m K]

The Biot Number has relevance to quenching because it deals with the conduction that is taking place within the metal sample as well as the conduction that is taking place at the surface of the part as the vapor layer convectively cools the part.

To use this dimensionless number for a cylinder, the characteristic length is the ratio of the surface area to the volume. In this ratio, we neglect end effects and simply calculate the surface area as the surface of the cylinder without the area of the ends. As a result, L = r/2 for the cylindrical probe that we are considering [19].

For bodies such as a cylinder, sphere, or plate, if Bi < 0.1, then the temperature at the center will not differ greatly from the temperature at the surface by more than 5% [18]. As a result, Bi < 0.1 is a suitable criterion for determining if the uniform temperature assumption is valid for a given part [18].

## 2.4 Quench Factor Analysis (QFA)

To successfully predict the metallurgical consequences of quenching, it is necessary to determine the heat transfer properties produced by the quenching medium during the cooling. Cooling curve analysis has been considered to be the best method to obtain such information [7]. Quench factor analysis (QFA) has several advantages over other methods. Quench factor analysis provides a single value describing quench severity for the specific alloy being quenched. In addition, the quench factor is directly related to the hardness of the quenched part and intermediate manual interpretations are not required. So, it can be seen that QFA is highly beneficial in the quenching process [4, 6-8, 10, 24].

To fully understand QFA, one must recognize that the rate of precipitation depends of both supersaturation and diffusion. These two factors are competing with each other as the temperature increases and decreases [6]. The two extremes allow for the slowest precipitation rate whereas intermediate temperatures result in the highest rates. At high temperatures, supersaturation is low, so the precipitation rate is low despite the high diffusion rate. And conversely, at low temperatures diffusion is low and supersaturation is high, but the precipitation rate is still low.

The determination of the Quench Factor, Q, begins with the calculation of a variable called the incremental quench factor ($\tau$). This variable is calculated for each time step in the cooling process and can be seen below in Equation 2.11.

$$\tau = \frac{\Delta t}{C_T} \tag{2.11}$$

$\tau$ = incremental quench factor
$\Delta t$ = time step used in cooling curve data acquisition

The $C_T$ function is defined below as well as the variables that help create it [4, 6-8, 10, 11, 24, 25].

$$C_T = -K_1 K_2 \exp\left[\frac{K_3 K_4^2}{RT(K_4 - T)^2}\right] \exp\left[\frac{K_5}{RT}\right] \quad \textbf{(2.12)}$$

Where:

$C_T$ = critical time required to form a constant amount of a new phase or reduce the hardness be a specific amount.
$K_1$ = constant which equals the natural logarithm of the fraction untransformed during quenching (the fraction defined by the TTP curve)
$K_2$ = constant related to the reciprocal of the number of nucleation sites
$K_3$ = constant related to the energy required to form a nucleus
$K_4$ = constant related to the solvus temperature
$K_5$ = constant related to the activation energy for diffusion
R = 8.3143 J/K mole
T = absolute temperature (K)

Values for the above constants were found experimentally by Totten, Bates and Jarvis [4]. The table below illustrates these constants for four different aluminum alloys.

| Alloy | K1 | K2 | K3 | K4 | K5 | Temp Range (deg C) |
|---|---|---|---|---|---|---|
| 7050-T76 | -0.00501 | 2.20E-19 | 5190 | 850 | 1.80E+05 | 425 - 150 |
| 7057-T6 | -0.00501 | 4.10E-13 | 1050 | 780 | 1.40E+05 | 425 - 150 |
| 2024-T851 | -0.00501 | 1.72E-11 | 45 | 750 | 3.20E+04 | 440 - 110 |
| 7075-T73 | -0.00501 | 1.37E-13 | 1069 | 737 | 1.37E+05 | 425 - 150 |

**Table 2.3:** K-Constants for Various Aluminum Alloys

Looking above, the values for K1, K3, and K4 are relatively consistent from alloy to alloy, but K2 is different by several orders of magnitude. This indicates that the number of nucleation sites present is much smaller for 2024-T851 than that of 7075 and

7050. In addition, 7050-T76 possesses the greatest number of sites since its value for K2 is by far the smallest.

The incremental quench factor ($\tau$), represents the ratio of the amount of time an alloy was held at a particular temperature divided by the time required for 1% transformation at that given temperature. This value is then summed over the entire transformation range to produce the cumulative quench factor (Q). The summation equation is seen below.

$$Q = \sum \tau = \sum_{T_1}^{T_2} \frac{\Delta t}{C_T} \quad \textbf{(2.13)}$$

In the above equation, the values of $T_1$ and $T_2$ are taken as the maximum and minimum temperature values, respectively, off of any TTP Curve. A typical TTP Curve is seen below and the location and values of $T_2$ and $T_1$ can be readily seen as well as how the $C_T$ function fits into the analysis [3, 7].

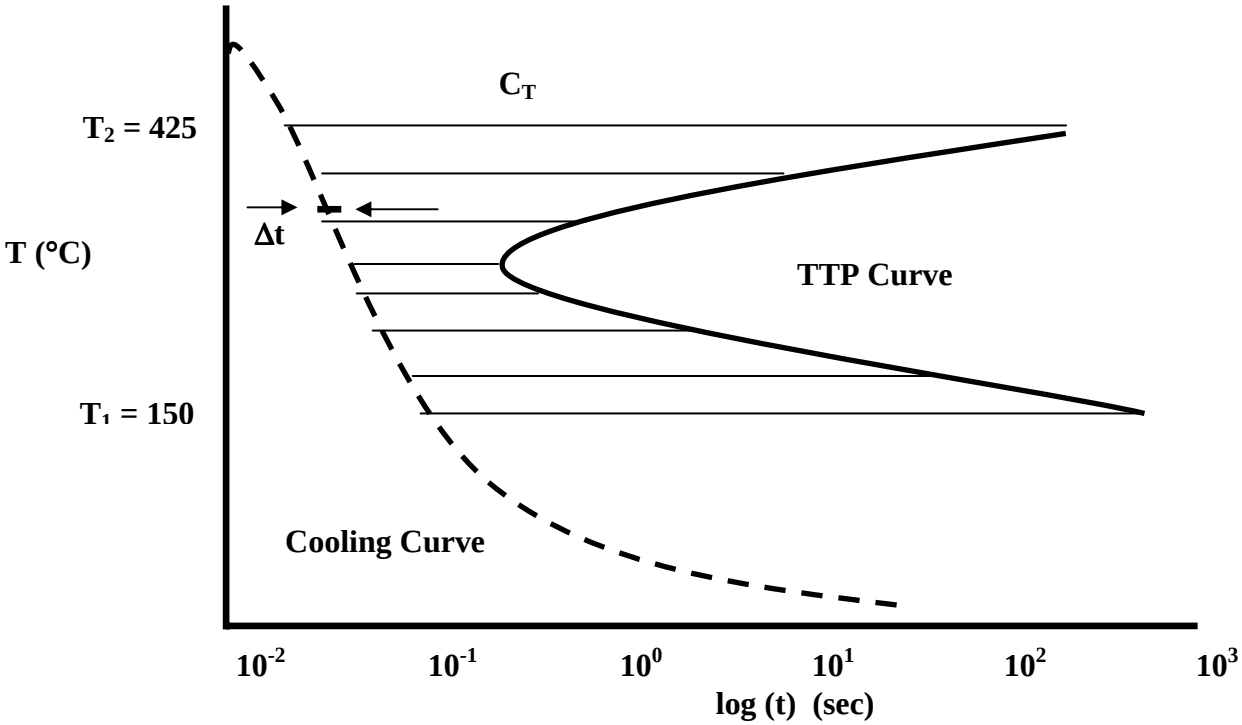


**Figure 2.9:** Cooling Curve and TTP Analysis

Above, the dashed line represents the cooling curve as the part is quenched and the corresponding TTP Curve is seen to its right. The Δt value is taken as the time interval in which data points are collected. In the second set of plots, it can be seen where the temperature from the cooling curve can be found on its corresponding TTP Curve. From these curves, the quench factor (Q) can be calculated as the summation of $\Delta t/C_T$. The quench factor is proportional to the heat removal characteristics of the quenchant as depicted in the cooling curve for the quenching process. The Q value is a single number that can classify the severity of the quench. This value can also be related to certain mechanical properties in materials such as hardness. A study has been done which correlated QFA to the hardness of an as-quenched 4130 steel [3]. Below in Figure 2.10, there is a plot of Q vs Rc, which shows the extent of the prediction. Looking at the curve below shows that the prediction is fairly accurate over a wide range of Rc values.

| QFA | Predicted Hardness | Measured Hardness |
|---|---|---|
| 7.2 | 51.8 | 52 |
| 12.4 | 50.9 | 51 |
| 18.5 | 49.4 | 50 |
| 25.6 | 48.8 | 50 |
| 33.1 | 47.7 | 49 |
| 41.5 | 46.4 | 47 |
| 50.1 | 45.2 | 45 |
| 58.7 | 44.1 | 42 |
| 67.3 | 43 | 42 |
| 86.8 | 40.7 | 39 |
| 103.1 | 38.9 | 38 |
| 119.1 | 37.3 | 36 |
| 134.8 | 35.8 | 35 |
| 150.1 | 34.5 | 34 |
| 175.3 | 32.5 | 33 |
| 197.6 | 31 | 31 |
| 215.6 | 29.9 | 30 |

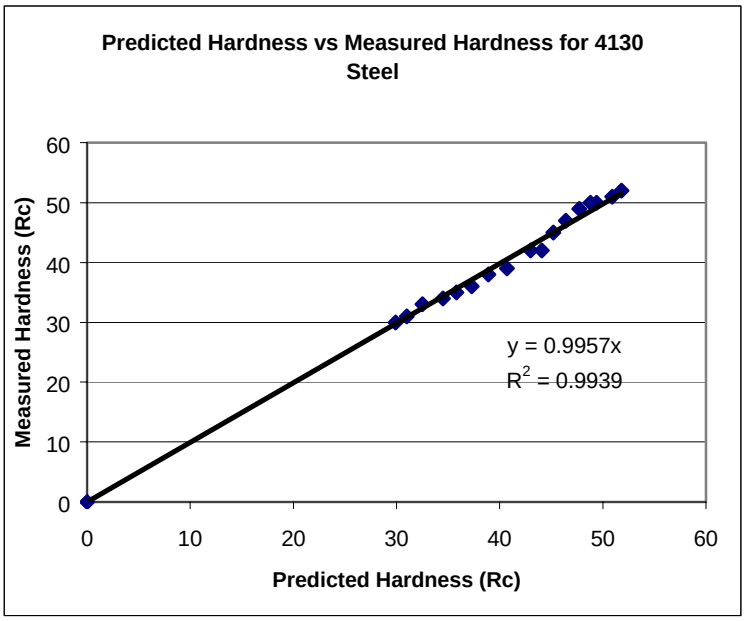


**Figure 2.10:** Correlation of QFA to Hardness of As-Quenched 4130 Steel [6]

As the cooling rate decreases, the QFA increases and can be used to predict the hardness of as-quenched materials. If this value is compared to the measured hardness, it is almost perfectly correlated. The plot on the right shows the extent of the correlation. The line of best fit is represented by the equation Y=0.9957X with an $R^2$ correlation of 0.9909. These two values indicate that QFA does an excellent job of predicting the hardness of as-quenched 4130 steel [6]. In addition, QFA has been correlated to mechanical properties such as yield strength, ultimate tensile strength and % elongation for 7057 aluminum alloys [5]. Having done so, it was shown that a QFA value of 20 or below allows for full properties to be achieved. If the QFA value exceeds 20, then the properties decrease considerably.

# 3.0 PROCEDURE

Aluminum probes, machined from 6061 aluminum, was quenched in distilled water while varying the initial bath temperature and amount of agitation to determine the effect each of these variables has on the overall quench severity. In order to fully understand the procedure used, it is important to have a good knowledge base of the equipment, experimental set-up, and metallurgical samples used during the quenching operation.

## 3.1 Experimental System

For the purpose of this research, the CHTE quench probe system was used [19, 26-29]. There are two main operations in the experiments, namely, heating and quenching. In the case of heating, a Thermolyne Model 1300 Box Furnace was used to heat the probe to the desired solutionizing temperature of 530°C. Once heating was complete, the probes were quenched in an aqueous bath contained in a Blue M, Model MW-1110A-1 Constant Temperature Bath Tank, which, in turn, was agitated by an Arrow 6000 Variable Agitation Unit. By introducing agitation into the system, it allows cooler bath water to be forced towards the part being quenched. As a result, the cooling rate will be increased and the degree of saturation of the material will be higher at the end of the quench [30].

The probe is connected to a coupling and connecting rod, both machined out of the same material, 6061 aluminum. The connecting rod is controlled by a pneumatic piston, which lowers the probe from inside the furnace to the quenching bath. A K-type thermocouple is inserted through the connecting rod down through the center of the

probe. This allows temperature data to be taken at the geometric center of the test piece. Below, Figure 3.1 shows a schematic of the quenching system.

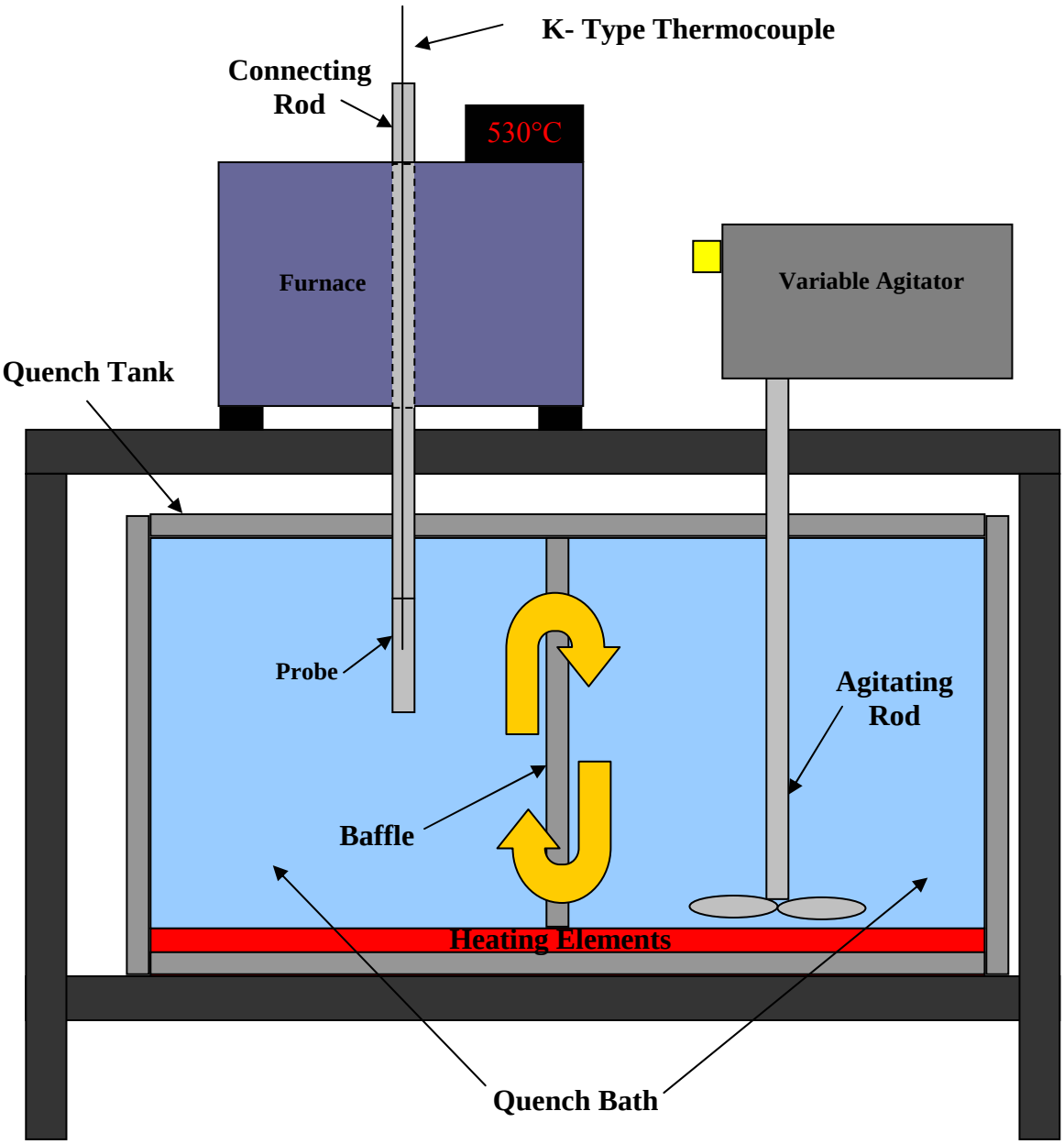


**Figure 3.1:** Schematic of Complete Agitation System

As seen from Figure 3.1, the bath is constantly mixed by the use of the variable agitation rod, which forces flow from the right side of the tank to the left side by the help of a baffle located in the center. The baffle is an H-shaped bracket that acts as an exit gate for water to be forced from the right side of the tank to the left and then a re-entry gate for water to return to the agitation side. The opening of the baffle is aligned with the agitation propeller to allow for a maximum degree of agitation flow.

## 3.2 Sample Preparation

The quenching experiments were conducted through the analysis of a standardized probe. The aluminum probes were machined based on the assumption of negligible temperature gradients within the system; that is to say, the temperature at the center of the probe does not vary from that at the surface. By using this negligible temperature gradient, we assume that the internal conductive resistance to heat transfer is small compared to the external convective resistance [18]. By doing so, a dimensionless number, the Biot Number (Bi), is created and mathematically defined as:

$$Bi = \frac{h_C L}{k_S}$$

*Where*: L = characteristic length (radius of cylinder/2)
$k_S$ = thermal conductivity of the solid
$h_C$ = conductive heat transfer coefficient

In order to use the lumped sum analysis, as presented in Section 2.3.2, we must ensure that for solids, such as a cylinder, Bi < 0.1. This value ensures that the temperature of the center will not differ from that of the surface by more than 5.0% [18]. As a result, the following dimensions were selected for the experimental probes.

**Figure 3.2:** CHTE Probe-Coupling Dimensions

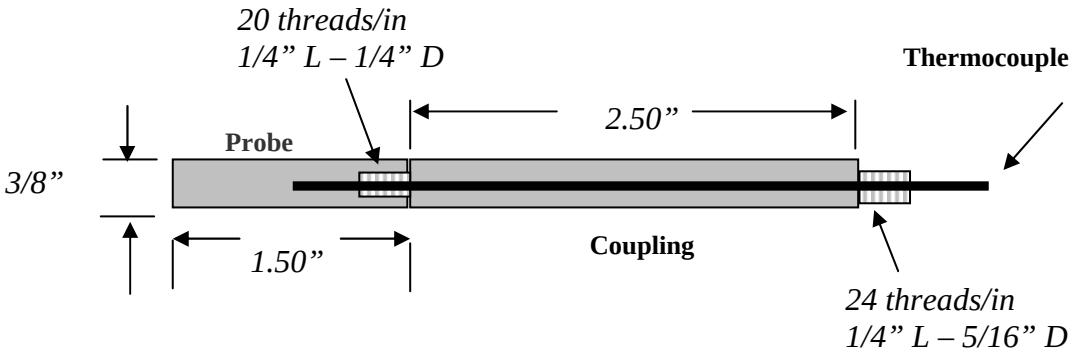


As mentioned previously, the thermocouple is located at the midpoint of the probe so the temperature data is taken at its geometric center. In addition to the Biot Number, the aspect ratio of length to diameter must be at least 4.0 in order to ignore end effects of the cylinder and solely concentrate on the heat transfer that is taking place radially at the location of the thermocouple [19].

In preparing the probe and coupling for actual experimentation, the interface where the probe connects to the coupling was sealed in order to eliminate the possibility of water leakage into the probe. Water leakage would cause the thermocouple to cool faster than the probe and result in inaccurate readings.

To solve this problem, Resbond 989, High-Purity Alumina Ceramic, purchased from Cotronics Corporation, was used to create the seal since it can be exposed to temperatures as high as 1650°C without melting. In addition, it is insoluble in water, so when quenched, the seal will remain in tact and not dissolve into the quenching medium. Below, Figure 3.3 illustrates a cross-sectional view of the probe-coupling set-up with the alumina paste seal.

**Figure 3.3:** Cross-Section of Probe-Coupling Interface with Alumina Seal and embedded Thermocouple

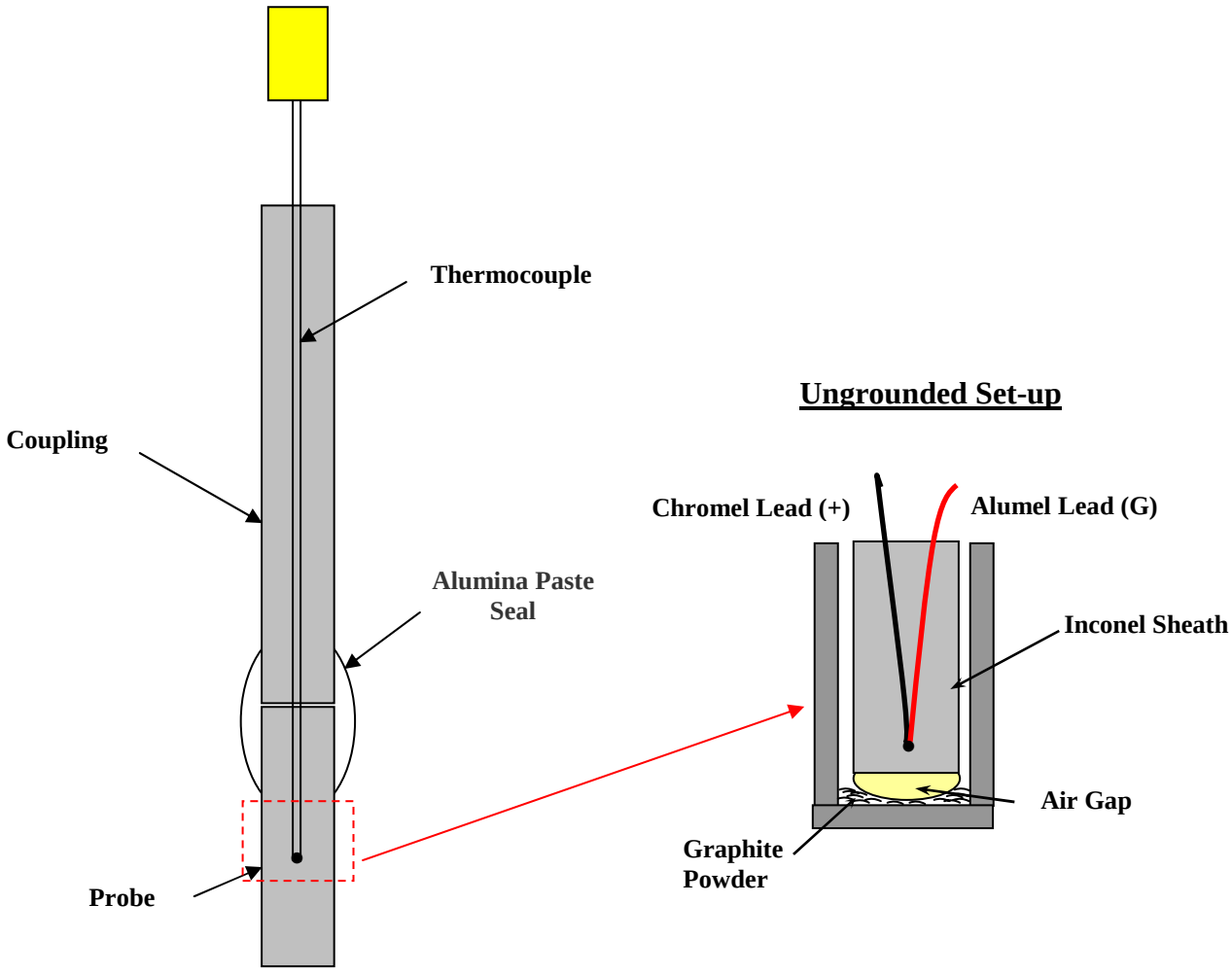


The alumina paste was applied and let air harden over night at room temperature. Once hard, it was further cured by baking in a box furnace for 4 hours at 200°C. This curing operation ensures the removal of all moisture within the alumina paste itself. As a result, the risk of the paste cracking is minimized.

To ensure an excellent electrical connection between the thermocouple and the probe, fine mesh graphite powder was placed in the hole of the probe where the thermocouple is embedded. As a result, better, continuous data will be collected during heating and quenching.

## 3.3 Conducting the Experiments

The CHTE probe is heated in the box furnace and held at the desired solutionizing temperature for five minutes. In the case of 6061 aluminum, ASM standards suggest a solutionizing temperature of 530°C [2, 16]. After the material has been successfully solutionized, the probe is lowered into the agitated bath by means of a pneumatic connecting rod. Once the rod begins its decent towards the quenching medium, it triggers the data acquisition software, LabVIEW, to begin recording the Time vs. Temperature cooling data.

After the completion of the quench, the probe is removed from the medium and sanded with 600-grit sand paper. The sanding is done after each quench in order to maintain a consistent surface finish of the probes as more experiments are carried out [19].

## 3.4 Test Matrix

A simple test matrix was devised for the experiments conducted in distilled water since there were only 2 quenching parameters that could be varied. The test matrix below lays out the conditions to be tested based on these parameters.

**Table 3.1:** Test Matrix for Quenching in Distilled Water

| Agitation Level (rpm) | | Bath Temperature (°C) | | | | |
|---|---|---|---|---|---|---|
| | | 5 | 25 | 40 | 80 | 100 |
| AG0 | 0 | X | X | X | X | X |
| AG1 | 880 | X | X | X | X | X |
| AG2 | 1850 | X | X | X | X | X |

Each ‘X’ represents 5 quenches at a given condition, so a total of 75 quenches will be completed. In the case of the distilled water bath, the testing parameters include

the agitation level and initial bath temperature. An agitation level of 0 indicates no agitation will be present, level 1 indicates a medium level of agitation classified by an impeller speed of 880 rpm and level 2 indicates a high degree of agitation classified by an impeller speed of 1850. As for the bath temperature, 5 distinct values were selected, namely: 5, 25, 40, 80, and 100°C. This variation will allow us to see the effect that initial bath temperature has on the quench.

## 3.5 Quench Factor Analysis Calculations

Once all the data from the test matrix was collected, a Quench Factor Analysis calculation was done to classify the severity of each quench. A spreadsheet was created which calculated the incremental quench factor parameter, $\tau$, based on the the cooling data (as described in Chapter 2.4 Quench Factor Analysis). In addition, the spreadsheet summed all the $\tau$ values over the testing range of 150°C - 425°C in order to create the single-number classification value, Q. These values were then compared for each quench criterion in order to characterize the severity of each quench.

## REFERENCES


1. Callister, W.D., *Materials Science and Engineering: An Introduction*. John Wiley and Sons, Inc, ed. t. Ed. 1997, New York.

2. ASM, ed. *Aluminum and Aluminum Alloys: ASM Specialty Handbook*., ed. J.R. Davis. 1993, ASM International.

3. ASM, *Quenching and Distortion Control*, ed. H.E. Boyer. 1998, Metals Park Ohio: ASM International.

4. Bates, C.E., L.M. Jarvis, and G.E. Totten, *Use of Quenching Factor for Predicting the Properties of Polymer Quenching Media.* Metal Science and Heat Treatment, 1996. **Vol. 38**(No. 5-6): p. 248-251.

5. Bates, C.E., T. Landig, and G. Seitanikis, *Quench Factor Analysis: A powerful Tool Comes of Age.* Heat Treating, 1985(December): p. 13-17.

6. Bates, C.E. and G.E. Totten. *Application of Quench Factor Analysis to Predict Hardness Under Laboratory and Production Condition*. in *Proceedings of the First International Conference on Quenching and Control of Distortion*. 1992 September. Chicago, Illinois.

7. Bates, C.E., G.E. Totten, and L.M. Jarvis, eds. *Quench Factor Analysis: Polymer vs. Hot Water*., ed. I. Tenaxol. 1994: Milwaukee, Wisconsin.

8. Bates, C.E., G.E. Totten, and G.M. Webster, *Cooling Curve and Quench Factor Characterization of 2024 and 7075 Aluminum Bar Stock Quenched in Type 1 Polymer Quenchants.* Heat Transfer Research, 1998. **Vol. 29**(No. 1-3).

9. Mackenzie, D.S. and G.E. Totten, *Aluminum Quenching Technology: A Review.* Materials Science Forum, 2000. **Vol. 331-337**: p. 589-594.

10. Bates, C.E., G.E. Totten, and N.A. Clinton, *Handbook of Quenchants and Quenching Technology*. 1993, Materials Park, Ohio: ASM International.

11. Staley, J.T., *Quench Factor Analysis of Aluminum Alloys*. 1987, The Institute of Metals: London, England. p. 923-934.

12. ASM, ed. *Aluminum: Vol. I Properties, Physical Metallurgy and Phase Diagrams*., ed. K.R. Van Horn. 1967, American Society of Metals International: Metals Park, Ohio.

13. http://cyberbuzz.gatech.edu/asm_tms/phase_diagrams/pd/al_mg.gif Georgia Technological University. 2002.

14. Totten, G.E. and G.M. Webster. *Cooling Curve Analysis - Data Acquisition*. in *Proceedings of the 16th ASM Heat Treating Society Conference and Exposition*. 1996 March. Cincinnati, Ohio.

15. Association, A., *International Alloy Designation and Chemical Composition Limits for Wrought Aluminum and Wrought Aluminum Alloys*. 2001 January, Unified North American and International Registration Records.

16. ASM, ed. *ASM Metals Reference Book, ASM International*. 3rd ed. ed., ed. M. Bauccio. 1993.

17. ASM, ed. *Aluminum: Vol. III Fabrication and Finishing*., ed. K.R. Van Horn. 1967, American Society of Metals International: Metals Park, Ohio.

18. Mills, A.F., *Heat Transfer*. 2nd Ed ed. 1999, Upper Saddle River, NJ,: Prentice Hall.

19. Chaves, J.C., *The Effect of Surface Finish Conditions and High Temperature Oxidation on Quenching Performance of 4140 Steel in Mineral Oil*. 2001 November 20, Worcester Polytechnic Institute.

20. Jarvis, L.M., G.E. Totten, and G.M. Webster. *Cooling Curve Analysis of Polymer Quenchants*. in *19th ASM Heat Treating Conference Proceedings Including Steel Heat Treating in the New Millennium*. 1999 November.

21. Totten, G.E. and G.M. Webster, *Cooling Curve and Quench Factor CHaracterization of 2024 and 7075 Aluminum Bar Stock Quenched in TYpe 1 Polymer Quenchants.* Heat Transfer Research, 1998. **Vol. 29**(No. 1-3): p. 163-175.

22. Purdue University, *Thermophysical Properties of Matter*. Specific Heat: Metallic Elements and Alloys, ed. Y.S. Touloukian. Vol. 4. 1970, New York: Purdue Research Foundation - Thermophysical Properties Research Center (TPRC).

23. Purdue University, *Thermophysical Properties of Matter*. Thermal Conductivity: Metallic Elements and Alloys. Vol. 1. 1970, New York: Purdue Research Foundation.

24. Bates, C.E., G.E. Totten, and G.M. Webster. *Aluminum Quenching with Polymer Quenchants: An Overview*. in *17th ASM Heat Treating Society Conference Proceedings Including the 1st International Induction Heat Treating Symposium*. 1997 September. Indianapolis, Indiana.

25. Bernardin, J.D. and I. Madawar, *Validation of the Quench Factor Technique in Predicting Hardness in Heat Treatable Aluminum Alloys.* International Journal of Heat and Mass Transfer, 1995. **Vol. 38**: p. 863-873.

26. Chaves, J.C., M. Maniruzzaman, and R.D. Sisson Jr. *A New Quench Characterization System for Steels*. in *Proceedings of the 21st Heat Treating Society Conference*. 2001. Indianapolis, Indiana.

27. Maniruzzaman, M., J.C. Chaves, and R.D. Sisson Jr. *CHTE quench probe system - a new quenchant characterization system*. in *5th International Conference on Frontiers of Design and Manufacturing*. 2002. Dalian, China.

28. Maniruzzaman, M. and R.D. Sisson Jr. *Investigation of bubble nucleation site density during quenching heat treatment process using video imaging*. in *TMS Annual Meeting 2002*. 2002. Seattle, WA.

29. Sisson, R.D. Jr, J.C. Chaves, and M. Maniruzzaman. *The Effect of Surface Finish on the Quenching Behavior of 4140 Steel in Mineral Oils*. in *Proceedings of the 21st Heat Treating Society Conference*. 2001. ndianapolis, Indiana.

30. Han, S.W., G.E. Totten, and S.G. Yun. *Continuously Variable Agitation in Quench System Design*. in *Proceedings From the First International Conference on Quenching and Control of Distortion*. 1992 September. Chicago, Illinois.

31. Bodin, J. and S. Segerberg. *Variation in the Heat Transfer Coefficients Around Components of Different Shapes During Quenching*. in *Proceedings From the First International Conference on Quenching and Control of Distortion,*. 1992 September. Chicago, Illinois.

32. Bodin, J. and S. Segerberg. *Experimental Difficulties of Achieving Reliable Cooling Curve Data*. in *Proceedings of the 16th ASM Heat Treating Society Conference and Exposition*. 1996 March. Cincinnati, Ohio.

33. Brimacombe, J.K., S.M. Gupta, and E.B. Hawbolt. *Determination of Quench Heat-Transfer Coefficients Using Inverse Methods*. in *Proceedings From the First International Conference on Quenching and Control of Distortion*. 1992 September. Chicago, Illinois.

34. Cano, J.F., R. Colas, and A. Garcia-Celias. *Aging in Heat Treatable Cast Aluminum Alloys". Of Polymer Quenchants*. in *The 1st International Automotive Heat Treating Conference*. 1998 July. Puerto Vallarta, Mexico.

35. Fuchizawa, S., M. Kogawara, and M. Narazaki. *Laboratory Test of Cooling Power of Polymer Quenchants*. in *Proceedings of the Second International Conference on Quenching and Control of Distortion*. 1996 November. Cleveland, Ohio.

36. Guisbert, D.A. *Precision and Accuracy of the Continuous Cooling Curve Test Method*. in *Proceedings of the 16th ASM Heat Treating Society Conference and Exposition*. 1996 March. Cincinnati, Ohio.

37. Guisbert, D.A. and D.L. Moore. *Influence of Test Conditions on the Cooling Cuve Response Of Polymer Quenchants*. in *19th ASM Heat Treating Conference Proceedings Including Steel Heat Treating in the New Millennium*. 1999 November.

38. Kearny, M.W., K.S. Lally., and G.E. Totten. *Quench Tank Agitation*. in *Proceedings From the First International Conference on Quenching and Control of Distortion*. 1992 September. Chicago, Illinois.

39. Krovit, *Selecting the Quenching Medium for Aluminum Alloys.* Metal Science and Heat Treatment., 1989 September. **Vol 31**(No. 3-4).

40. Lainer, K. and H.M. Tensi. *Determination of Vapor Film Thickness During Immersion Cooling in Aqueous Polymer Solutions*. in *Proceedings of the Second International Conference on Quenching and Control of Distortion*. 1996 November. Cleveland, Ohio.

41. Ness, A.R. and V. Sverdin. *Solution Treatment of High Strength Aluminum Alloys in the Aerodynamic Heat Treat Furnace (AHTF)*. in *The 1st International Automotive Heat Treating Conference*. 1998 July. Puerto Vallarta, Mexico.

42. Sverdlin, A.V., G.E. Totten, and G.M. Webster, *Quenching Media Based on Polyalkylene Glycol for Heat Treatment of Aluminum Alloys.* Metal Science and Heat Treatment, 1996. **Vol. 38**(No. 5-6): p. 252-254.

43. Sverdlin, A.V., G.E. Totten, and G.M. Webster, *Use of the Quenching Factor for Predicting the Properties of Polymer Quenching Media.* Metal Science and Heat Treatment, 1996. **Vol. 38**(No. 5-6).

44. Tensi, H.M. and G.E. Totten. *Industrial Polymer Quenchants - Determination of Cooling Characteristics - Laboratory Test Methods*. in *Proceedings of the 16th ASM Heat Treating Society Conference and Exposition*. 1996 March. Cincinnati, Ohio.

45. Maniruzzaman, M. and R.D. Sisson Jr. *Bubble Dynamics During Quenching of Steel*. in *ASM Heat Treating Society*. 2001. Indianapolis, Indiana.

## 4.0 PUBLICATIONS

This chapter contains two papers that have been submitted for publication. The papers present all of the results that were collected through this research.

The first paper entitled, “The Effect of Temperature and Agitation Level on the Quench Severity of 6061 Aluminum in Distilled Water”, written by M. Fontecchio, M. Maniruzzaman, and R.D. Sisson, Jr. describes the effect of quenching parameters through quenching 6061 aluminum in distilled water. This article was submitted to the American Society of Metals’ (ASM) 13th Annual International Federation for Heat Treatment & Surface Engineering (IFHTSE) Congress. The second article entitled, “Quench Factor Analysis and Heat Transfer Coefficient Calculation for 6061 Aluminum Alloy Probed Quenched in Distilled Water”, written by M. Fontecchio, M. Maniruzzaman, and R.D. Sisson, Jr. presents a comparison of QFA and heat transfer coefficients calculations in 6061 aluminum probes. This article was submitted to “Journal of Materials Processing Technology”.

# The Effect of Bath Temperature and Agitation Rate on the Quench Severity of 6061 Aluminum in Distilled Water

**Marco Fontecchio, Mohammed Maniruzzaman and Richard D. Sisson, Jr.**

Center for Heat Treating Excellence
Materials Science and Engineering Program, Mechanical Engineering Department
Worcester Polytechnic Institute (WPI), Worcester, MA 01609

## Abstract

A 6061 aluminum probe was quenched with a CHTE probe-quenching system in distilled water while varying bath temperature and the level of agitation. Time vs. temperature data was collected during the quench by use of an ungrounded K-type thermocouple embedded inside the probe, while cooling rates were calculated. A Quench Factor Analysis (QFA) was also performed to quantitatively classify the quench severity. The data showed an increase in maximum cooling rate as bath temperature decreased and agitation level increased. In addition, it was found that at higher levels of agitation, there was also an increase in the standard deviation of the cooling rate.

## Introduction

The main goals of this work are to experimentally determine the effect of bath temperature and agitation rate of the quenching medium on cooling behavior and Quench Factor, Q [1].

Understanding how quenching parameters affect the outcome of the quench is important for control of mechanical properties as well as elimination of distortion and cracking [2]. In many cases, cold water (10-32°C) is typically used in the quenching of aluminum alloys, but cold water occasionally produces unacceptable distortion due to high thermal gradients that exist in the part. If this problem exists, the part can be quenched in hot water (60-70°C) to reduce these thermal gradients and eliminate the

possibility of cracking [3]. However, the slower cooling may reduce the mechanical properties obtained after heat treating.

The time-temperature cooling associated with the rapid quenching of the material can be controlled through the variation of the quenching parameters such as the bath temperature and agitation level. For example, as the temperature of the bath increases, there is more of a tendency for the vapor blanket stage to be prolonged due to the nature of water to form vapor as it approaches the boiling point [4]. The obvious disadvantage is that the cooling rate will be slower and the desired mechanical properties may not be achieved. Aside from distortion, uneven hardness and soft-spot distribution can be seen with a water quench when the vapor blanket is prolonged and encourages vapor and bubble entrapment in certain locations. Because of this, uneven heat transfer will be experienced throughout the part and consequently, soft-spots can develop in these areas [5].

The second parameter of interest is the agitation level. In general, agitation increases the rate of heat transfer throughout the quenching process regardless of the bath temperature. Agitation will breakdown the vapor blanket much earlier in the quench and force the transition to nucleate boiling [2]. As a result, a stage of slow cooling is cut short and replaced with a stage of rapid heat transfer. In addition, agitation will also produce smaller, more frequent bubbles during the Boiling Stage, which, in turn, creates faster rates of heat transfer throughout the part [3]. Finally, agitation forces cool liquid to constantly be circulated to the workpiece in place of the hot liquid at the surface of the part [2]. Therefore, higher temperature differences will always exist between the medium and the surface, resulting in faster rates of heat dissipation [6].

## Quench Factor Analysis (QFA)

Quench factor analysis (QFA) provides a single value that quantitatively classifies quench severity for a specific alloy [1, 7-13]. QFA is an analysis of the cooling curve associated with a particular quench coupled with a Time Temperature Property (TTP) curve defined by Eq. 2 below [1, 7-13]. The analysis begins with calculation of a variable called the incremental quench factor ($\tau$), which is performed for each time step in the cooling process.

$$\tau = \frac{\Delta t}{C_T}$$

$\tau$ = incremental quench factor
$\Delta t$ = time step used in cooling curve data acquisition

**Eq. 1**

The $C_T$ function is defined below in Eq. 2 as well as the variables that help create it [1, 7, 8, 10, 11, 13-15]

$$C_T = -K_1 K_2 \exp\left[\frac{K_3 K_4^2}{RT(K_4 - T)^2}\right] \exp\left[\frac{K_5}{RT}\right] \qquad \textbf{Eq. 2}$$

Where:
$C_T$ = critical time required to form a constant amount of a new phase or reduce the hardness be a specific amount.
$K_1$ = constant which equals the natural logarithm of the fraction untransformed during quenching (typically 99.5%: (ln (0.995)) = -0.00501
$K_2$ = constant related to the reciprocal of the number of nucleation sites
$K_3$ = constant related to the energy required to form a nucleus
$K_4$ = constant related to the solvus temperature
$K_5$ = constant related to the activation energy for diffusion
R = 8.3143 J/K mole
T = absolute temperature (K)

The incremental quench factor ($\tau$) above, represents the ratio of the amount of time an alloy was held at a particular temperature divided by the time required for 1% transformation at that given temperature. This value is then summed over the entire

transformation range to produce the cumulative quench factor (Q). The summation equation is seen below.

$$Q = \sum \tau = \sum_{T_1}^{T_2} \frac{\Delta t}{C_T} \qquad \textbf{Eq. 3}$$

In Equation 3, the values of $T_1$ and $T_2$ are taken as the maximum and minimum temperature values, respectively, off of any TTP Curve. A typical TTP Curve is seen below and the location and values of $T_2$ and $T_1$ can be readily seen as well as how the $C_T$ function fits into the analysis [2, 10]. For the purpose of this analysis, $T_1$ and $T_2$ are equal to 150°C and 425°C, respectively [1].

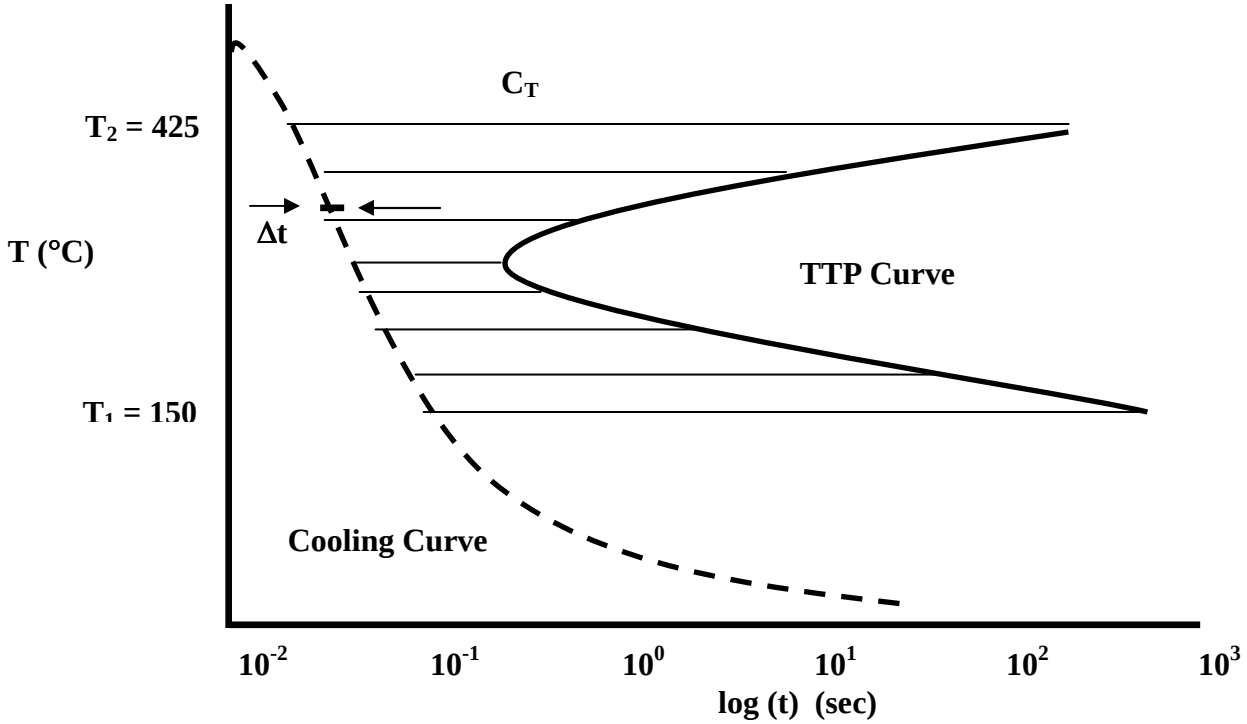


**Figure 1: Cooling Curve and TTP Curve Analysis[9]**

Above, the dashed line represents the temperature of the alloy as a function of time and the corresponding TTP Curve is seen to its right. The Δt value is taken as the

time interval in which data points are collected. From these curves, the quench factor (Q) can be calculated as the summation of $\Delta t/C_T$. The quench factor is proportional to the heat removal characteristics of the quenchant as depicted in the cooling curve for the quenching process [9]. The Q value can classify the severity of the quench for a particular alloy. The cooling rate is inversely proportional to QFA, that is to say, the greater the cooling rate, the smaller the quench factor, Q.

## Experimental Procedure

The quenching system used in this analysis is composed of a modified box furnace, constant temperature bath tank and variable agitation unit [16-20]. The constant temperature bath tank heated and maintained 12 liters of distilled water while the agitation was induced via a 2.5-inch diameter impeller located on one side of the quench tank. The impeller forced fluid to flow from one side of the tank to the other with the help of a baffle located in the center of the tank.

The test piece, a CHTE probe and coupling machined out of 6061 aluminum is shown below in Figure 2.

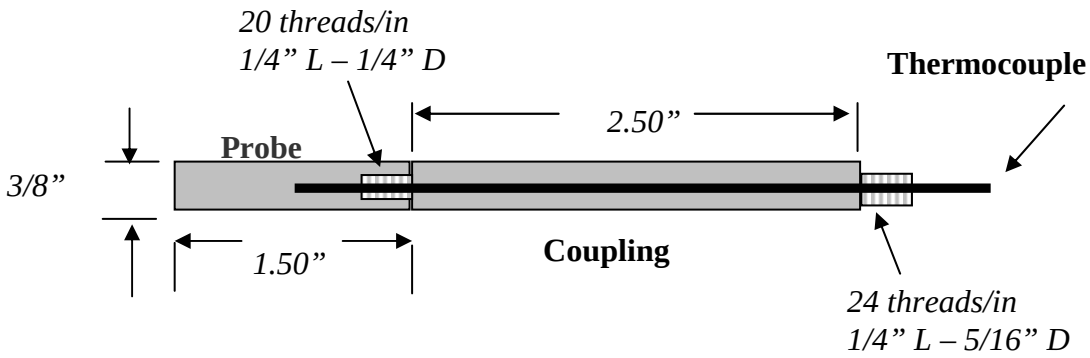


**Figure 2: Probe-Coupling Dimensions**

An ungrounded K-type thermocouple was embedded in the center of the probe, in order to take temperature data at its geometric center. In addition, graphite powder was placed in the center of the probe to maintain an excellent electrical contact between the test piece and thermocouple. Initially, a grounded K-type thermocouple was used, but created several data acquisition problems due to an electrochemical reaction between the sheath of the thermocouple and the center of the aluminum probe. The switch to the ungrounded thermocouple alleviated these problems and allowed for the collection of smooth, continuous data.

In order to eliminate the possibility of water leaking into the probe center, Resbond 989, High-Purity Alumina Ceramic, purchased from Cotronics Corporation, was applied to the interface between the probe and coupling. Once applied, it was air hardened for 4 hours then baked at 200C for 4 hours to insure proper curing and decrease the risk of cracking.

| Agitation Rate (rpm) | Water Temperature (deg C) | | | | |
|---|---|---|---|---|---|
| | 5 | 25 | 40 | 80 | 100 |
| 0 | X | X | X | X | X |
| 880 | X | X | X | X | X |
| 1850 | X | X | X | X | X |

**Table 1: Distilled Water Test Matrix**

In terms of agitation rate, at 880 rpm, the flow in the quench tank appears to be lamellar, whereas at 1850 rpm, the flow is highly agitated and assumed to be turbulent.

The fluid velocity at the location of the probe could not be measured; therefore, the Reynolds number could not be calculated to quantify the fluid flow.

Five quenching experiments were performed for each condition. Once all quenches were complete, cooling rates and quench factor analysis were conducted.

## Results

As presented by the test matrix above, each condition was tested 5 times. Once collected, the cooling rate data from each curve was averaged and plotted to see the variation of cooling rates as a function of water temperature and agitation. Below, Figures 3-5 show this variation for each level of agitation. Important aspects to note on these figures are the fact that as the temperature of the water decreases, the maximum cooling rate increases. The maximum cooling rates at 5°C, 25°C, and 40°C are relatively close in magnitude, but as the temperature of the water is increased further, there is a considerable decrease in maximum cooling rate. In addition, as the temperature approaches 80°C, a Liedenfrost point becomes visible on each plot indicating that the probe is being alternatively covered with a vapor blanket and liquid layer resulting in oscillating surface temperatures [18]. Furthermore, the temperature at which the maximum cooling rate occurs is much lower than that of the other bath temperatures. The same trend is observed at 100°C, but with an even lower maximum cooling rate temperature.

In addition, as the three figures are compared, it can be seen that as the level of agitation increases, the maximum cooling rates at each temperature increase. This trend is observed in each corresponding temperature of the bath. This increase can be due in part to the constant recirculation of cool bath water to the quenched part during the

cooling process, as well as the mechanical breakdown of the vapor layer stage at the start of the quench [3].

The final important aspect of these three plots is the maximum cooling rate ranges that can be achieved. At an agitation level of 0, values that range from 40°C/s to 105°C/s can be achieved whereas at levels 1 and 2, ranges of 50°C/s to 140°C/s and 60°C/s to 190° C/s can be achieved, respectively.

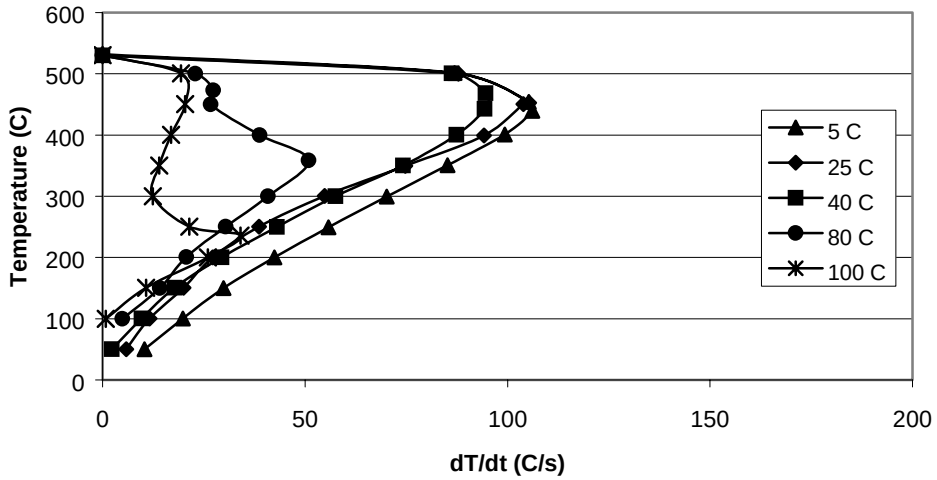


**Figure 3: Average Cooling Curves at Various Temperatures with No Agitation**

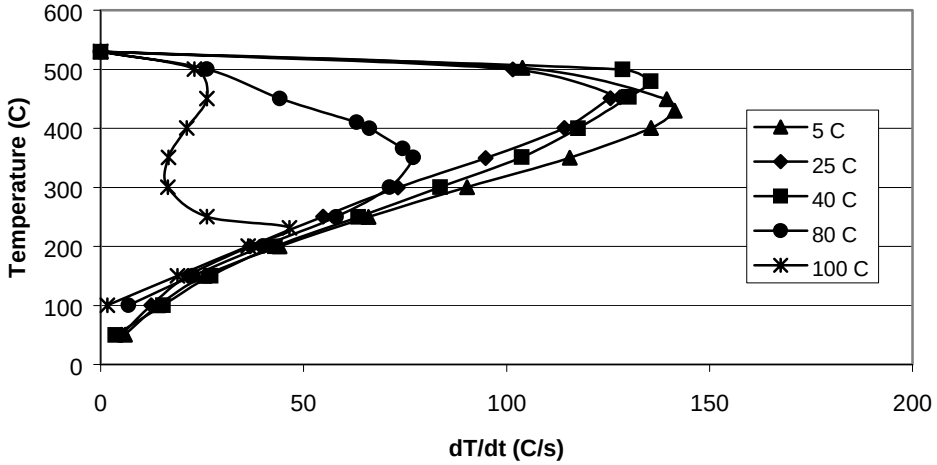


**Figure 4: Average Cooling Curves at Various Temperatures at 880 rpm**

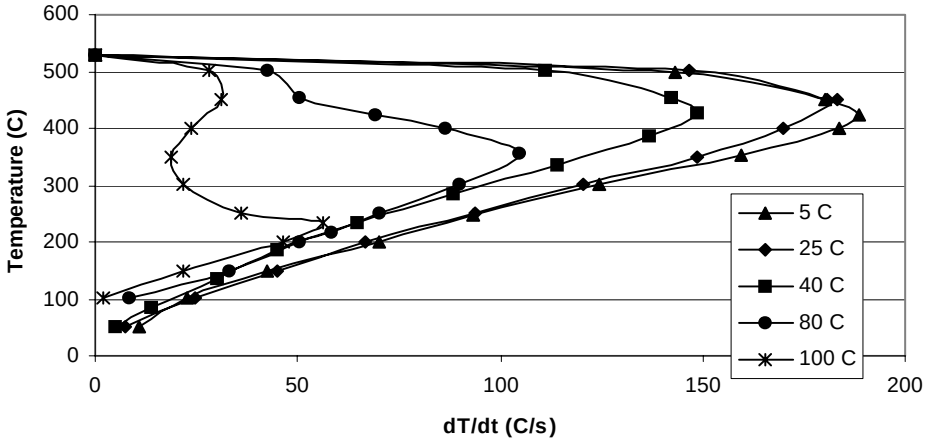


**Figure 5: Average Cooling Curves at Various Temperatures at 1850 rpm**

In addition to cooling curves, quench factor analysis was completed to quantify the severity of the quench. Table 2 presents the maximum cooling rates at a given condition as well as the quench factor, Q. Looking at the table, it is clear to see that within each temperature region, the quench factor decreases as the agitation level increases. In terms of a cooling curve, it indicates that the quench was performed at a faster rate, which is also supported by the maximum cooling rate in the second row. As mentioned previously, and supported here, the cooling rate increases with decreased water temperature and increased agitation. So, the quench factor does a good job at quantifying the quench based on maximum cooling rate information.

| | Bath Temperature (deg C) | | | | | | | | | | | | | | |
|---|---|---|---|---|---|---|---|---|---|---|---|---|---|---|---|
| | 5 | | | 25 | | | 40 | | | 80 | | | 100 | | |
| | AG0 | AG1 | AG2 | AG0 | AG1 | AG2 | AG0 | AG1 | AG2 | AG0 | AG1 | AG2 | AG0 | AG1 | AG2 |
| T max | 439 | 429 | 422 | 452 | 452 | 449 | 468 | 479 | 427 | 358 | 365 | 354 | 235 | 231 | 232 |
| dT/dt max | 106 | 141 | 188 | 105 | 127 | 182 | 94 | 135 | 148 | 50 | 74 | 104 | 34 | 46 | 56 |
| QFA (Q) | 6.82 | 5.27 | 3.78 | 8.31 | 6.45 | 4.67 | 8.26 | 5.86 | 5.21 | 12.5 | 7.51 | 6.18 | 40.6 | 32.97 | 29.52 |

**Table 2: Maximum Cooling Rates and Quench Factor Q as a Function of Water Temperature and Agitation Level**

## Statistical Variation in Cooling Rate With Increasing Agitation

In conducting these experiments, it is important to note that there existed a wide variation in the experimental data as the temperature and agitation level increased. Table 3 presents the standard deviation of the cooling rate associated with each quench condition. The experimental data shows that as agitation level increases, the variation in the data also increases; that is to say that at lower levels of agitation, the variation in the data is smaller, but as the agitation is increased, the variation increases. Table 3 shows that at all bath temperature, the standard deviation increases with increasing agitation level. Furthermore, looking at Table 4, it can be seen that the ratio of standard deviation to the mean cooling rate also increases with increasing agitation rate. This range can be attributed to the nature of the agitated flow. It could be possible that the turbulent flow at higher agitation levels was not a true circular flow, but rather interfered with itself and caused the warmer water to remain in contact with the part and not be circulated away. In addition, there could be entrapped gas within the agitated water. As a result, as the water is circulated towards the probe, the gas would essentially be quenchiung the part and not the fresh, cooler bath water. This cooling rate would be slower since the heat capacity of air is much less that that of water. That is to say that it would take more

energy to heat water than it would to heat gas and as a result, the cooling power of water with entrapped gas is much less than that of water [6].

| Agitation Level (rpm) | | Bath Temperature (deg C) | | | | |
|---|---|---|---|---|---|---|
| | | 5 C | 25 C | 40 C | 80 C | 100 C |
| AG0 | 0 | 6.278 | 10.278 | 7.822 | 5.828 | 3.955 |
| AG1 | 880 | 12.080 | 13.211 | 12.143 | 14.752 | 7.281 |
| AG2 | 1850 | 18.562 | 35.894 | 21.217 | 16.770 | 10.551 |

**Table 3: Standard Deviation of Maximum Cooling Rate as a Function of Agitation Level and Bath Temperatures**

| Agitation Level (rpm) | | Bath Temperature (deg C) | | | | |
|---|---|---|---|---|---|---|
| | | 5 C | 25 C | 40 C | 80 C | 100 C |
| AG0 | 0 | 0.179 | 0.271 | 0.218 | 0.247 | 0.335 |
| AG1 | 880 | 0.195 | 0.337 | 0.265 | 0.397 | 0.455 |
| AG2 | 1850 | 0.216 | 0.432 | 0.349 | 0.267 | 0.488 |

**Table 4: Ratio of Standard Deviation to Maximum Cooling Rate as a Function of Agitation Level at Different Bath Temperatures**

## Conclusions

Based on the experimental data presented above, it can be concluded that:

- An increase in agitation causes an increase in cooling rate and a decrease in Quench Factor, Q.
- 
- A decrease in bath temperature causes an increase in cooling rate and a decrease in Quench Factor, Q.
- 
- The standard deviation and range of the cooling rates at all temperatures increases with agitation
- 
- The Quench Factor, Q, appears to be an excellent parameter for characterizing the quenching system (i.e. the quenching fluid and the alloy being quenched)

## References


1. Bates, C.E., T. Landig, and G. Seitanikis, *Quench Factor Analysis: A powerful Tool Comes of Age.* Heat Treating, 1985(December): p. 13-17.

2. ASM, *Quenching and Distortion Control*, ed. H.E. Boyer. 1998, Metals Park Ohio: ASM International.

3. Mackenzie, D.S. and G.E. Totten, *Aluminum Quenching Technology: A Review.* Materials Science Forum, 2000. **Vol. 331-337**: p. 589-594.

4. Hasson, J. *Quenchants: Yesterday, Today, and Tomorrow*. in *Proceedings of the First International Conference on Quenching and Control of Distortion*. 1992 September. Chicago, Illinois.

5. ASM, ed. *Aluminum and Aluminum Alloys: ASM Specialty Handbook*., ed. J.R. Davis. 1993, ASM International.

6. Mills, A.F., *Heat Transfer*. 2nd Ed ed. 1999, Upper Saddle River, NJ,: Prentice Hall.

7. Bates, C.E., L.M. Jarvis, and G.E. Totten, *Use of Quenching Factor for Predicting the Properties of Polymer Quenching Media.* Metal Science and Heat Treatment, 1996. **Vol. 38**(No. 5-6): p. 248-251.

8. Bates, C.E. and G.E. Totten. *Application of Quench Factor Analysis to Predict Hardness Under Laboratory and Production Condition*. in *Proceedings of the First International Conference on Quenching and Control of Distortion*. 1992 September. Chicago, Illinois.

9. Bates, C.E., G.E. Totten, and L.M. Jarvis, eds. *Quench Factor Analysis: Polymer vs. Hot Water*., ed. I. Tenaxol. 1994: Milwaukee, Wisconsin.

10. Bates, C.E., G.E. Totten, and G.M. Webster, *Cooling Curve and Quench Factor Characterization of 2024 and 7075 Aluminum Bar Stock Quenched in Type 1 Polymer Quenchants.* Heat Transfer Research, 1998. **Vol. 29**(No. 1-3).

11. Bernardin, J.D. and I. Madawar, *Validation of the Quench Factor Technique in Predicting Hardness in Heat Treatable Aluminum Alloys.* International Journal of Heat and Mass Transfer, 1995. **Vol. 38**: p. 863-873.

12. Staley, J.T., *Effect of Quench Path on Properties of Aluminum Alloys.* JTS Alcoa Laboratories.: p. 396-407.

13. Staley, J.T., *Quench Factor Analysis of Aluminum Alloys*. 1987, The Institute of Metals: London, England. p. 923-934.

14. Bates, C.E., G.E. Totten, and N.A. Clinton, *Handbook of Quenchants and Quenching Technology*. 1993, Materials Park, Ohio: ASM International.

15. Bates, C.E., G.E. Totten, and G.M. Webster. *Aluminum Quenching with Polymer Quenchants: An Overview*. in *17th ASM Heat Treating Society Conference Proceedings Including the 1st International Induction Heat Treating Symposium*. 1997 September. Indianapolis, Indiana.

16. Chaves, J.C., M. Maniruzzaman, and J.R.D. Sisson. *A New Quench Characterization System for Steels*. in *Proceedings of the 21st Heat Treating Society Conference*. 2001. Indianapolis, Indiana.

17. Maniruzzaman, M., J.C. Chaves, and R.D. Sisson. *CHTE quench probe system - a new quenchant characterization system*. in *5th International Conference on Frontiers of Design and Manufacturing*. 2002. Dalian, China.

18. Maniruzzaman, M. and R.D. Sisson Jr. *Bubble Dynamics During Quenching of Steel*. in *ASM Heat Treating Society*. 2001. Indianapolis, Indiana.

19. Maniruzzaman, M. and R.D. Sisson Jr. *Investigation of bubble nucleation site density during quenching heat treatment process using video imaging*. in *TMS Annual Meeting 2002*. 2002. Seattle, WA.

20. Sisson, R.D. Jr., J.C. Chaves, and M. Maniruzzaman. *The Effect of Surface Finish on the Quenching Behavior of 4140 Steel in Mineral Oils*. in *Proceedings of the 21st Heat Treating Society Conference*. 2001. ndianapolis, Indiana.

# Quench Factor Analysis and Heat Transfer Coefficient Calculations for 6061 Aluminum Alloy Probes Quenched in Distilled Water

**Marco Fontecchio, Mohammed Maniruzzaman and Richard D. Sisson, Jr.**
Center for Heat Treating Excellence
Materials Science and Engineering Program, Mechanical Engineering Department
Worcester Polytechnic Institute (WPI), Worcester, MA 01609

## Abstract

A 6061 aluminum probe was quenched with a CHTE probe-quenching system in distilled water while varying bath temperature and the level of agitation. Time vs. temperature data was collected during the quench by use of an ungrounded K-type thermocouple embedded inside the probe. Heat transfer coefficients were calculated via a Newtonian Cooling Analysis and Quench Factor Analysis (QFA) was performed for each experiment to quantitatively classify the quench severity. Heat transfer coefficient values ranged from 1000 $W/m^2K$ to 3900 $W/m^2K$. The data also showed that at higher levels of agitation and lower bath temperatures, the maximum heat transfer coefficient increased, while the Quench Factor, Q, decreased.

## Introduction

The main goal of this work is to calculate the heat transfer coefficient, 'h' as a function of temperature as well as make comparisons with Quench Factor Analysis for aluminum alloys. The quenching conditions were varied to obtain a wide range of cooling rates for the data analysis.

Understanding how quenching parameters affect the outcome of the quench is important for control of mechanical properties as well as elimination of distortion and cracking [1]. In many cases, cold water (10-32°C) is typically used in the quenching of

aluminum alloys, but cold water occasionally produces unacceptable distortion due to high thermal gradients that exist in the part. If this problem exists, the part can be quenched in hot water (60-70°C) to reduce these thermal gradients and eliminate the possibility of cracking [2]. However, the slower cooling may reduce the mechanical properties obtained after heat-treating.

The time-temperature cooling associated with the rapid quenching of the material can be controlled through the variation of the quenching parameters such as the bath temperature and agitation level. For example, as the temperature of the bath increases, there is more of a tendency for the vapor blanket stage to be prolonged due to the nature of water to form vapor as it approaches the boiling point [3]. The obvious disadvantage is that the cooling rate will be slower and the desired mechanical properties may not be achieved. Aside from distortion, uneven hardness and soft-spot distribution can be seen with a water quench since the vapor blanket is prolonged and will encourage vapor and bubble entrapment in certain locations. Because of this, uneven heat transfer will be experienced throughout the part and consequently, soft spots can develop in these areas [4].

The second parameter of interest is the agitation level. In general, agitation increases the rate of heat transfer throughout the quenching process regardless of the bath temperature. Agitation will breakdown the vapor blanket much earlier in the quench and force the transition to nucleate boiling [1]. As a result, a stage of slow cooling is cut short and replaced with a stage of rapid heat transfer. In addition, agitation will also produce smaller, more frequent bubbles during the Boiling Stage, which, in turn, creates faster rates of heat transfer throughout the part [2]. Finally, agitation forces cool liquid to

constantly be circulated to the workpiece in place of the hot liquid at the surface of the part [1]. Therefore, higher temperature gradient will always exist between the medium and the surface, resulting in faster rates of heat dissipation [5].

## Stages of Quenching

Quenching takes place in three distinct stages, namely: Vapor Blanket Stage, Boiling Stage, and Convective Stage. The Vapor Blanket Stage begins when the hot part makes contact with the quenching medium. As the part is submersed, an unbroken vapor blanket surrounds the piece. This blanket exists because the supply of heat from the surface of the part exceeds the amount of heat needed to form the maximum vapor per unit area on the piece [6]. This stage is characterized by a relatively slow cooling rate since the vapor of the quenching medium surrounds the part and acts as an insulator. In this particular stage, heat is removed from the part by radiation and conduction through the vapor layer. As the component cools, the vapor blanket cannot be maintained and therefore breaks down. After this breakdown, the Boiling Stage immediately begins. The surface of the part is now in direct contact with the fluid and results in violent boiling of the medium. This stage is characterized by rapid heat transfer. As the part continues to cool below the boiling point of the medium, the Boiling Stage can no longer exist and it too breaks down giving way to the Convective Stage. This stage, much like the Vapor Blanket Stage, is also characterized by slow rates of heat transfer. Heat is dissipated from the part by movement of the quenching medium by conduction currents. The difference in temperature between the boiling point of the medium and actual temperature of the medium is the major factor influencing the rate of heat transfer in liquid quenchants [6]. Furthermore, viscosity of the medium at this point also affects the

cooling rate since a less viscous medium will dissipate heat faster than one of high viscosity [5].

Figure 1 presents the stages of quenching as seen on a typical cooling curve acquired during quenching. Also seen on this figure is the corresponding cooling rate curve associated with the quench. The slope of the cooling curve between the stages is the cooling rate, so it can easily be seen that the Vapor Layer Stage and Convection Stage have slow cooling rates since the slope of the line at those points is small. On the other hand, the slope of the Boiling Stage is quite large and therefore, the cooling rate is high.

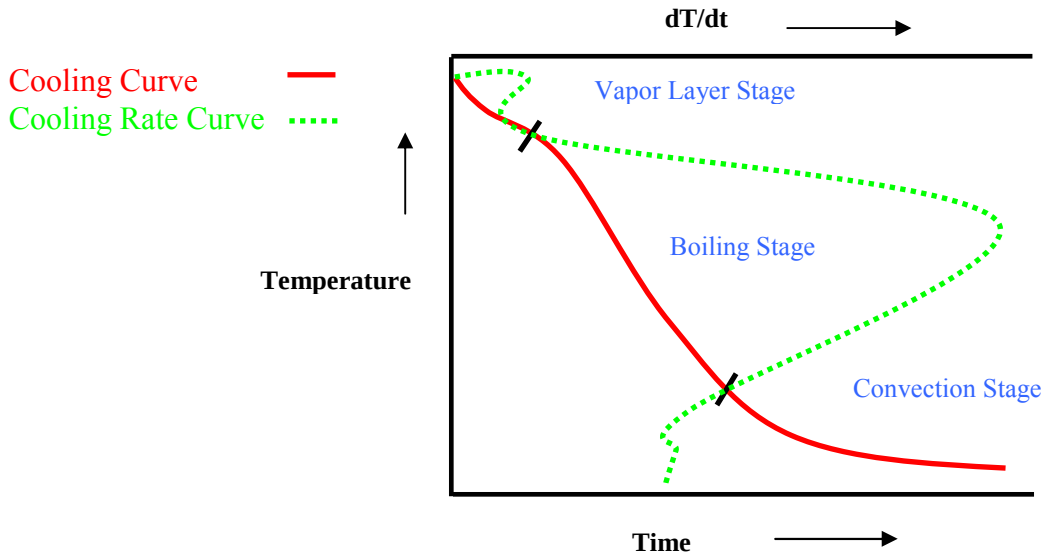


**Figure 1: Typical Cooling Curve with Corresponding Cooling Rate and Stages of Quenching**

## Heat Transfer Coefficient Calculations

The heat transfer coefficient '*h*' [W/ $m^2$ K] during quenching can be calculated by an inverse method [7]. This procedure is done by calculating the cooling rate (dT/dt) that is taking place in the part, and then using it to calculate the heat transfer coefficient '*h*'.

Since time and temperature curves are continually collected via data acquisition software, the cooling rate is calculated by taking the derivative of the cooling curve.

Newtonian Cooling (i.e. lumped sum analysis) will be used in our calculations [5].

$$h = \frac{V\rho(T)c_p(T)\frac{dT}{dt}}{A(T_s - T_l)} \quad \textbf{(1)}$$

$T_s$ = temperature of the part [K]
$T_l$ = temperature of the quenching liquid [K]
A = surface area of the part being quenched [$m^2$]
V = Volume of Part [$m^3$]

Equation 1 is derived from convective properties of the medium with respect to the quenched body. The V/A ratio is a constant (0.238 m) and equal to the radius of the test probe divided by two. Both density (ρ) and specific heat ($c_p$) of the material as a function of temperature during the quench were used to increase the accuracy of the calculation. Below, Figure 2 presents the dependency of $c_p$ on temperature for various aluminum alloys.

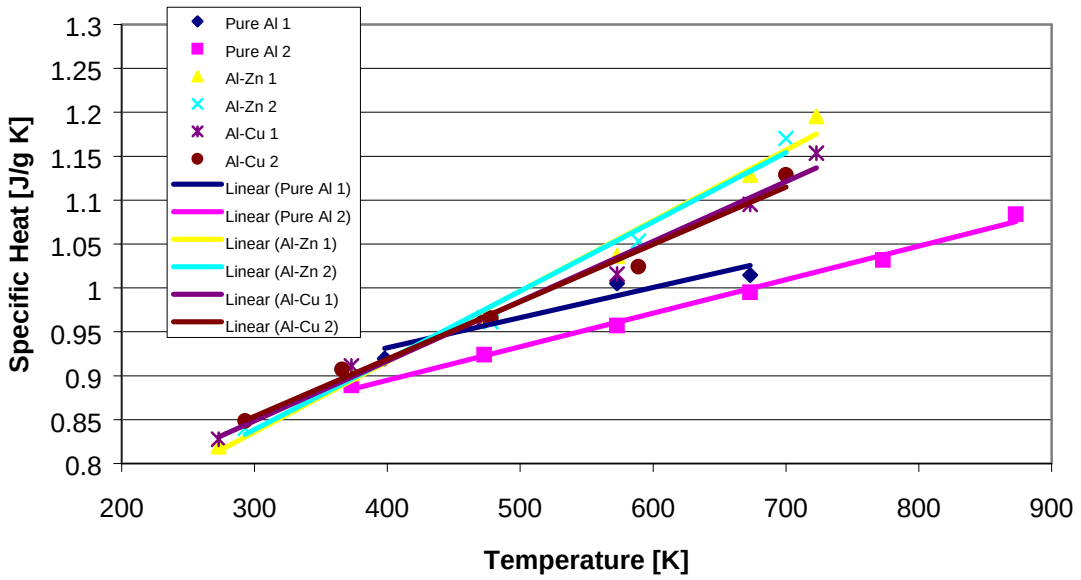


**Figure 2: Specific Heat as a Function of Temperature for Various Aluminum Alloys** [8]

It can be seen that the lines of best fit for the four alloys all lie directly on each other whereas the curves for pure aluminum deviate from the alloys at higher temperatures. For this reason, it was assumed that the specific heat of 6061 aluminum will follow a similar trend as the other alloys presented within the figure. In addition, the specific heat of 6061 aluminum at room temperature is equal to 0.896 J/Kg K, which falls directly on the line of best fit above. For these reasons, it will be assumed that 6061 will follow similar trends at higher temperatures and this curve, with an equation of Cp [J/KgK] = 0.007T + 0.644, will be used in our heat transfer coefficient calculations.

In addition, the density of the material can be determined as a function of temperature. The density of the material is not constant because the volume of the part will increase with increasing temperature. The linear coefficient of thermal expansion, $\alpha$, for 6061 aluminum is equal to 2.26 x $10^{-6}$ /K [4]. Equation 2 illustrates the formula used in calculating this variation at elevated temperatures.

$$\rho = \frac{m}{(l_o + l_o \alpha \Delta T)(d_o + d_o \alpha \Delta T)^2} \quad \textbf{(2)}$$

m = mass of probe [g]
$\alpha$ = Coefficient of thermal expansion [cm/cmK]
$l_o$ = Initial length of probe at room temp [cm]
$d_o$ = Initial diameter of probe at room temp [cm]
$\Delta T$ = Change in temperature ($T_{part}$ - 273) [K]

The variation in density over the temperature range of interest is quite small. The values range from 1.875 g/cm$^3$ to 1.94 g/cm$^3$, which is a variation of only 1.7% about the mean [4]. For this reason, it will be assumed that the density is constant and an average value equal to 1.905 g/cm$^3$ will be used in our calculations.

## Quench Factor Analysis (QFA)

Quench factor analysis (QFA) provides a single value that quantitatively classifies quench severity for a specific alloy [9-16]. QFA is an analysis of the cooling curve associated with a particular quench coupled with a Time Temperature Property (TTP) curve defined by Eq. 4 below [9-16]. The analysis begins with calculation of a variable called the incremental quench factor ($\tau$), which is performed for each time step in the cooling process.

$$\tau = \frac{\Delta t}{C_T} \qquad \textbf{(3)}$$

$\tau$ = incremental quench factor
$\Delta t$ = time step used in cooling curve data acquisition

The $C_T$ function is defined below in Eq. 4 as well as the variables that help create it [6, 9-11, 13, 14, 16, 17]

$$C_T = -K_1 K_2 \exp\left[\frac{K_3 K_4^2}{RT(K_4 - T)^2}\right]\exp\left[\frac{K_5}{RT}\right] \qquad \textbf{(4)}$$

Where:
$C_T$ = critical time required to form a constant amount of a new phase or reduce the hardness be a specific amount.
$K_1$ = constant which equals the natural logarithm of the fraction untransformed during quenching (typically 99.5%: (ln (0.995)) = -0.00501
$K_2$ = constant related to the reciprocal of the number of nucleation sites
$K_3$ = constant related to the energy required to form a nucleus
$K_4$ = constant related to the solvus temperature
$K_5$ = constant related to the activation energy for diffusion
R = 8.3143 J/K mole
T = absolute temperature (K)

The values of the constants used in this research were found in literature and shown below in Table 1.

| K1 | K2 | K3 | K4 | K5 |
|---|---|---|---|---|
| -0.00501 | 2.20E-19 | 5190 | 850 | 1.80E+05 |

**Table 1: K-Constant Values for Quench Factor Analysis[12]**

The incremental quench factor ($\tau$) above, represents the ratio of the amount of time an alloy was held at a particular temperature divided by the time required for 1% transformation at that given temperature. This value is then summed over the entire transformation range to produce the cumulative quench factor (Q). The summation equation is seen below.

$$Q = \sum \tau = \sum_{T_1}^{T_2} \frac{\Delta t}{C_T} \qquad \textbf{(5)}$$

In Equation 5, the values of $T_1$ and $T_2$ are taken as the maximum and minimum temperature values, respectively, off of any Time-Temperature-Property (TTP) Curve. A typical TTP Curve is seen below and the location and values of $T_2$ and $T_1$ can be readily seen as well as how the $C_T$ function fits into the analysis [1, 13]. For the purpose of this analysis, $T_1$ and $T_2$ are equal to 150°C and 425°C, respectively [10].

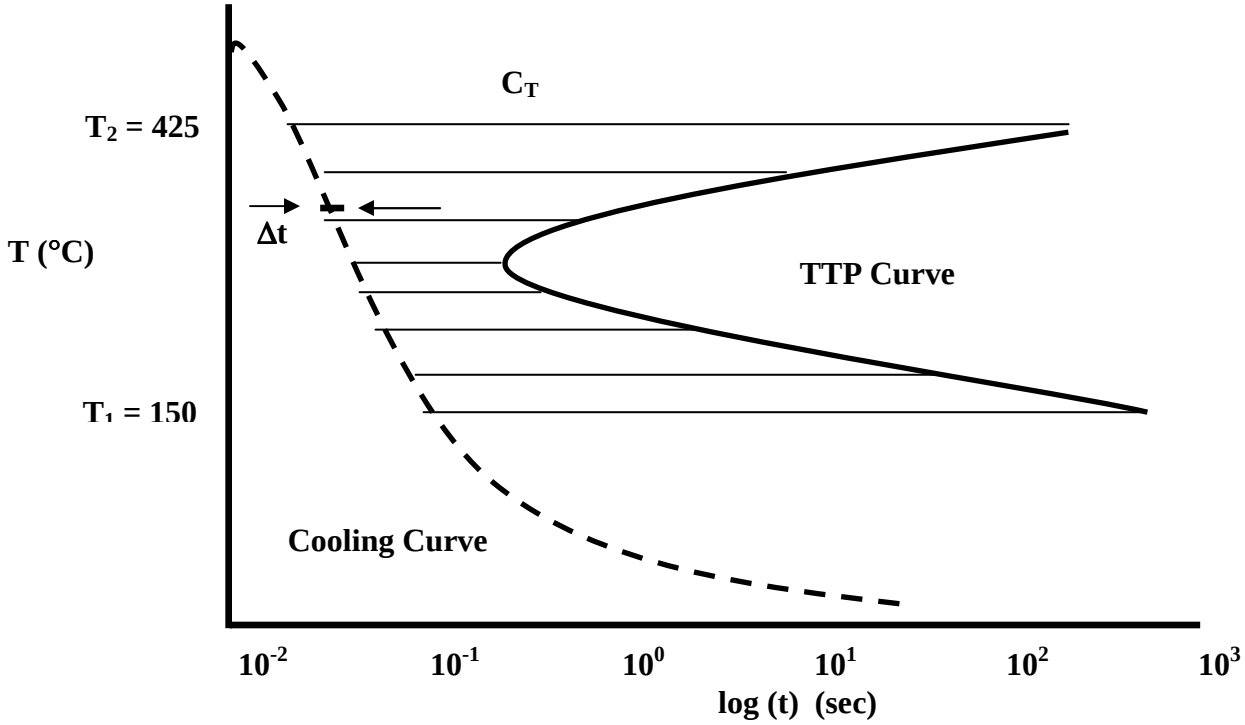


**Figure 3: Cooling Curve and TTP Curve Analysis[12]**

Above, the dashed line represents the temperature of the alloy as a function of time and the corresponding TTP Curve is seen to its right. The Δt value is taken as the time interval in which data points are collected. From these curves, the quench factor (Q) can be calculated as the summation of $\Delta t/C_T$. The quench factor is proportional to the heat removal characteristics of the quenchant as depicted in the cooling curve for the quenching process [12]. The Q value can classify the severity of the quench for a particular alloy. The cooling rate is inversely proportional to QFA, that is to say, the greater the cooling rate, the smaller the quench factor, Q.

## Experimental Plan

To determine the effect of bath temperature and agitation level on heat transfer coefficients and QFA, the following test matrix was created. Table 2 lays out the conditions to be tested. Each bath temperature will be tested with each corresponding agitation level, so a total of 15 conditions will be explored. Five samples were quenched at each test condition to determine the repeatability of the quench.

| Agitation Rate (rpm) | Water Temperature (°C) | | | | |
|---|---|---|---|---|---|
| | 5 | 25 | 40 | 80 | 100 |
| 0 | X | X | X | X | X |
| 880 | X | X | X | X | X |
| 1850 | X | X | X | X | X |

**Table 2: Distilled Water Test Matrix**

The agitation rate will be quantified by the rotations per minute of the immersed impeller. The fluid velocity at the location of the probe could not be measured; therefore, the Reynolds number could not be calculated to quantify the fluid flow. At 880 rpm, the flow in the quench tank appears to be lamellar, whereas at 1850 rpm, the flow is highly agitated and appears to be turbulent.

## Experimental Procedure

The test piece, a CHTE probe and coupling machined out of 6061 aluminum is shown below in Figure 4 [18-21].

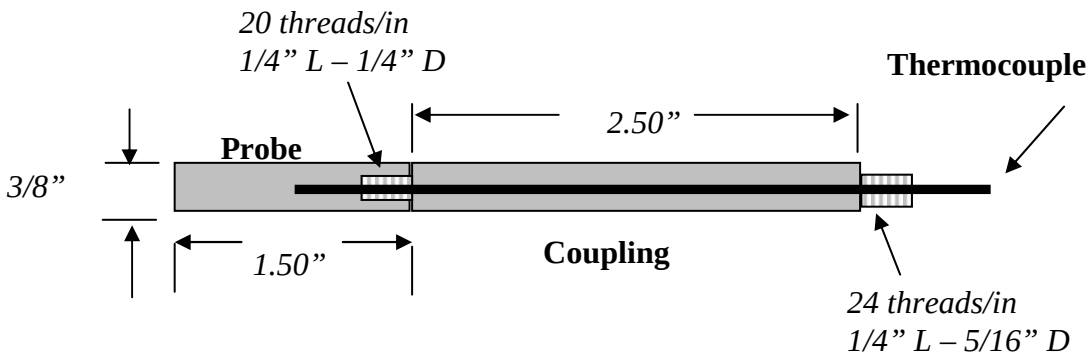


**Figure 4: Probe-Coupling Dimensions**

An ungrounded K-type thermocouple was embedded in the center of the probe, in order to take temperature data at its geometric center. In addition, graphite powder was placed in the center of the probe to maintain an excellent electrical contact between the test piece and thermocouple. Initially, a grounded K-type thermocouple was used, but created several data acquisition problems due to an electrochemical reaction between the sheath of the thermocouple and the center of the aluminum probe. The switch to the ungrounded thermocouple alleviated these problems and allowed for the collection of smooth, continuous data.

In order to eliminate the possibility of water leaking into the probe center, Resbond 989, High-Purity Alumina Ceramic, purchased from Cotronics Corporation, was applied to the interface between the probe and coupling. Once applied, it was air hardened for 4 hours then baked at 200°C for 4 hours to insure proper curing and decrease the risk of cracking.

This probe was used in conjunction with a CHTE probe quench system in order to conduct the experiments. The CHTE quenching system is composed of a modified box furnace, constant temperature bath tank and variable agitation unit [18-23]. Figure 5 is a schematic of the system illustrating the location of each component and the nature of the agitated fluid.

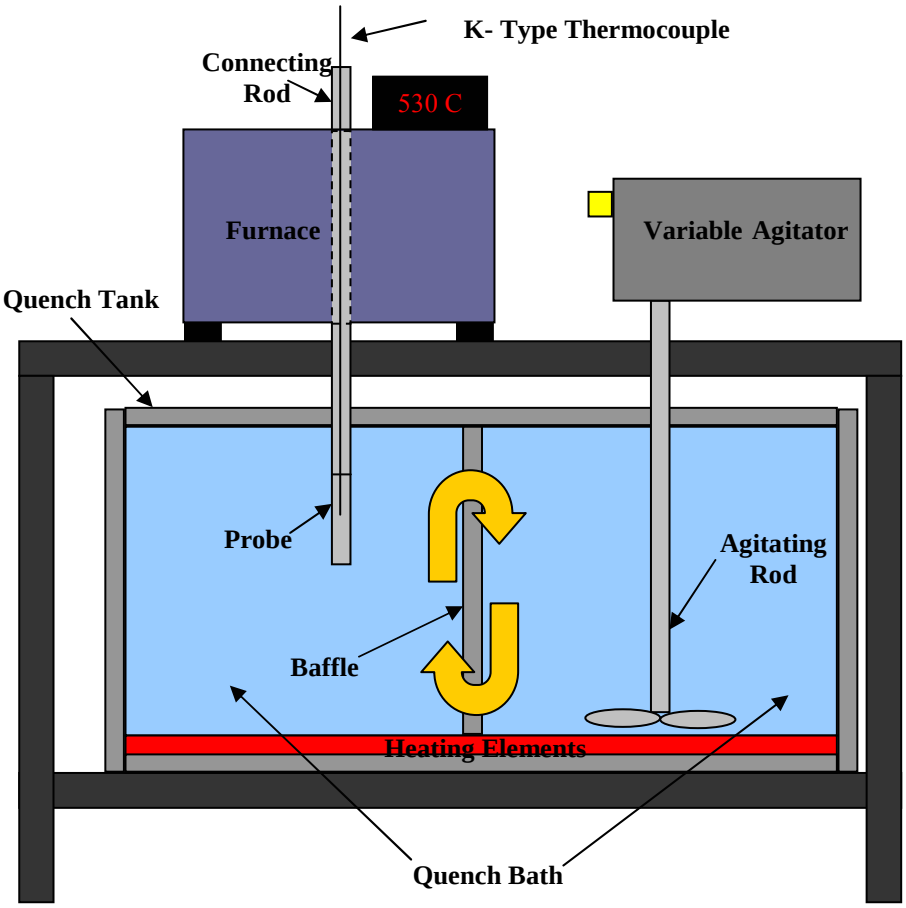


**Figure 5: Schematic of CHTE Quench System**

The probe is connected to a coupling and connecting rod, both machined out of the same material, 6061 aluminum. The connecting rod is controlled by a pneumatic piston, which lowers the probe from inside the furnace to the quenching bath. The probe is solutionized to 530°C before quenching in the distilled water quenching tank. The bath

is 12 liters in volume and its temperature is controlled by the variable heating elements located on the tank floor.

The bath is constantly mixed by the use of the variable agitation rod, which forces flow from the right side of the tank to the left side with the help of a baffle located in the center. The baffle is an H-shaped bracket that acts as an exit gate for water to be forced from the right side of the tank to the left and then a re-entry gate for water to return to the agitation side. The opening of the baffle is aligned with the agitation propeller to allow for a maximum degree of agitation flow.

Once the probe is lowered from inside the furnace, a switch triggers a data acquisition to begin collecting time-temperature data from the embedded thermocouple at a rate of 1000 data points per second. From start to finish, 40,000 data points are collected. The data is then reduced to 1000 data points by a smoothing operation by taking a running average of the data. Furthermore, the derivative (dT/dt) of the data is taken in order to analyze the cooling rates associated with each quench condition. The derivative is calculated by use of a four-point numerical method [24]. Equation 6 shows the equation that was used focused around data point 3 in the time-temperature data collected during the quench.

$$\frac{dT}{dt} = \frac{T_1 - 8T_2 + 8T_4 - T_5}{12\Delta t} \qquad \text{(6)}$$

$\Delta t$ = time difference between data points
T = temperature at a given data point

Once all experiments were completed, heat transfer coefficients and Quench Factor Analysis was performed for each quench condition.

## Experimental Results: Heat Transfer Coefficients

Heat transfer coefficients were calculated using Equation 1. The data from each of the five quench experiments was averaged and plotted below in Figures 6 through 8. These three figures illustrate the change in 'h' as a function of initial bath temperatures for each of the three agitation levels. Figure 6 demonstrates that as the bath temperature increased, the effective heat transfer coefficient decreases. The curves for 5°C and 25°C are relatively similar in magnitude starting at 530°C until 460°C where the curve at 5°C achieves higher 'h' values. In addition, as the temperature approaches 80°C and 100°C, a Liedenfrost point becomes clearly visible on each plot indicating that the probe is being alternatively covered with a vapor blanket and liquid layer which causes oscillating surface temperatures [23]. Furthermore, at 100°C, the Liedenfrost point is prolonged much further before the maximum 'h' value is achieved. As a result, the temperature at which the maximum 'h' value occurs decreases from 360°C to 225°C. The low temperature gradient between the quenching medium and the hot 6061 probe may stabilize film boiling before leading into nucleate boiling, thus causing this decrease in temperature [23].

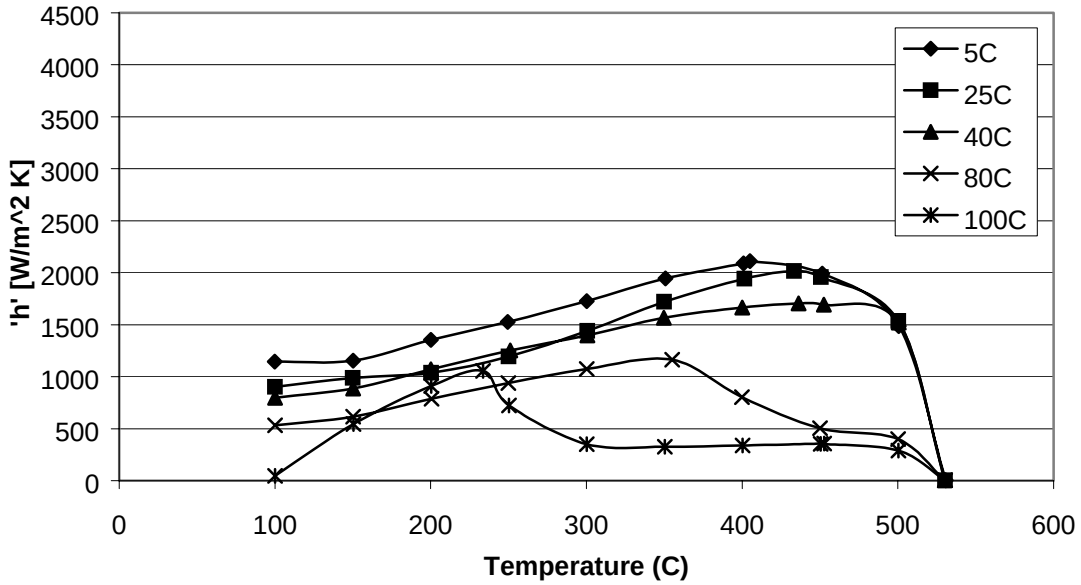


**Figure 6: Effective Heat Transfer Coefficients for Various Temperatures With No Agitation**

Figures 7 and 8 show similar trends that were observed in Figure 6, except the presence of the Leidenfrost point does not appear in the curves for 80°C. It is believed that since agitation is now present, the fluid flow mechanically broke down the vapor layer and promoted nucleate boiling. As a result, film boiling could not become stable and, therefore, does not appear on either curve [25].

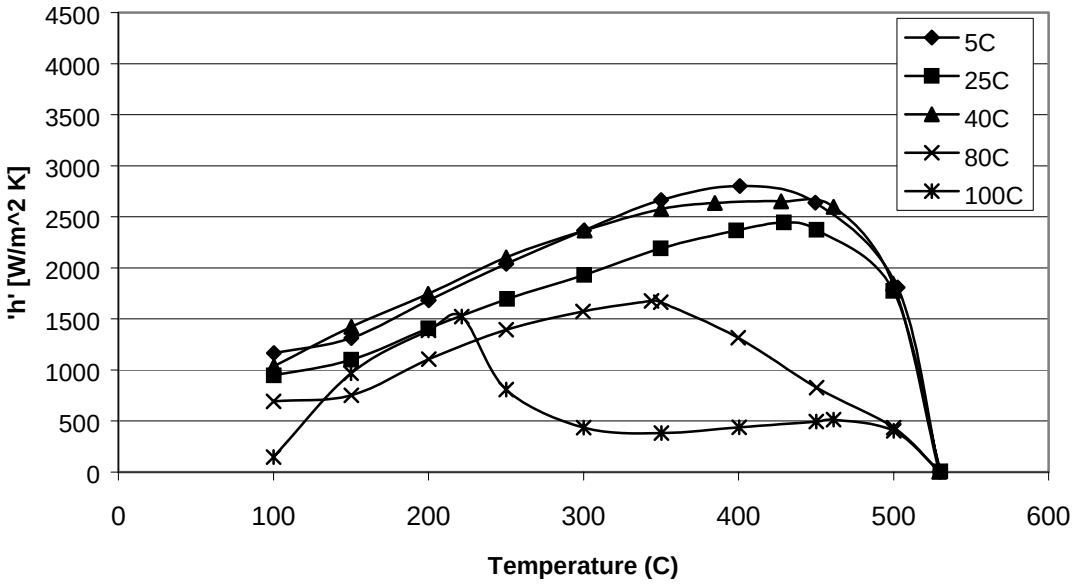


**Figure 7: Effective Heat Transfer Coefficients for Various Temperatures With An Agitation Level of 880 rpm**

The final noteworthy aspect of these three figures is the maximum heat transfer coefficient that is attainable for each condition. At an agitation rate of 0 rpm, values that range from 1100 $W/m^2K$ to 2100 $W/m^2K$ can be achieved whereas at agitation rates of 880 and 1850 rpm, ranges of 1500 $W/m^2K$ to 2800 $W/m^2K$ and 2000 $W/m^2K$ to 3850 $W/m^2K$ can be achieved, respectively

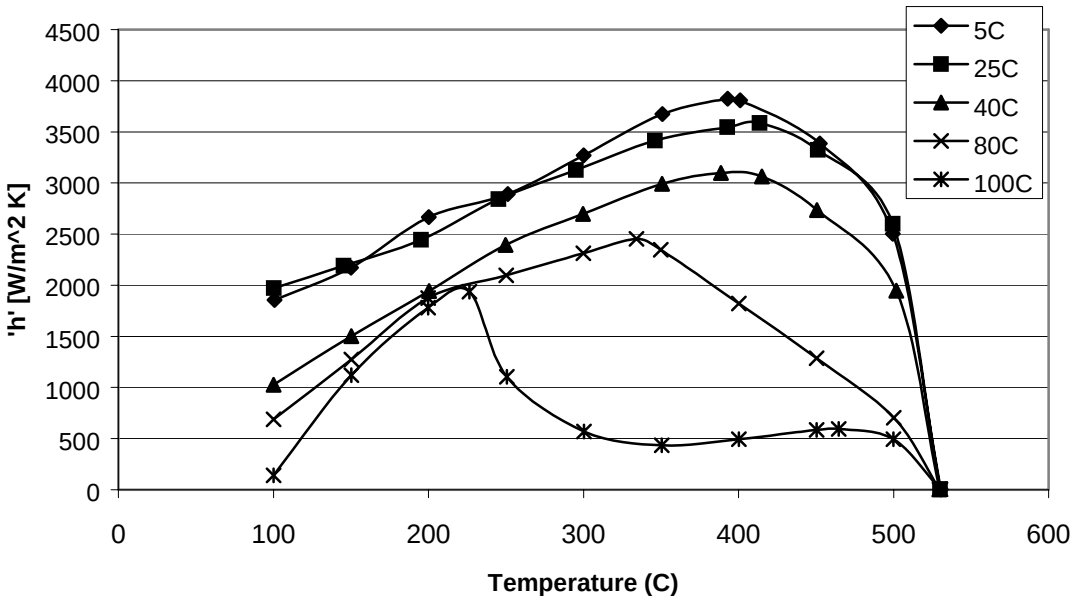


**Figure 8: Effective Heat Transfer Coefficients for Various Temperatures With An Agitation Level of 1850 rpm**

## Experimental Results: Quench Factor Analysis (QFA)

Using Equation 5, Quench Factor Analysis (QFA) was performed. Table 3 presents the Quench Factor, Q, for each quench condition. Looking down the columns of the table, it can be seen that Q decreases with increasing agitation level, indicating that the quench rate increases with increasing agitation. In addition, Q increases with increasing bath temperature as seen by the increasing values across the rows of the table. Overall, the fastest quench rate was observed at 5°C with an agitation level of 1850 rpm and the slowest at 100°C with no agitation. The Q values for these conditions are equal to 3.78 and 40.6, respectively.

| Agitation Level (rpm) | | Temperature C | | | | |
|---|---|---|---|---|---|---|
| | | 5 | 25 | 40 | 80 | 100 |
| AG0 | 0 | 6.82 | 8.31 | 8.26 | 12.5 | 40.6 |
| AG1 | 880 | 5.27 | 6.45 | 5.86 | 7.51 | 32.97 |
| AG2 | 1850 | 3.78 | 4.67 | 5.21 | 6.18 | 29.52 |

**Table 3: Variation in Quench Factor as a Function of Agitation and Bath Temperature**

Figure 9 plots the data presented in Table 3 against the corresponding maximum heat transfer coefficient seen in Figures 6 through 8. A hyperbolic curve was fit to the data, but looking at the $R^2$ value, the relationship does not appears to be hyperbolic since $R^2 = 0.49$. Overall, there is a general trend of higher maximum heat transfer coefficients at lower values of Q. The greatest value of maximum heat transfer coefficient was obtained at the same condition as the lowest Q value from Table 3. This data is consistent with theory since it is understood that low temperature and high agitation should yield high rates of heat transfer and low values in QFA [1].

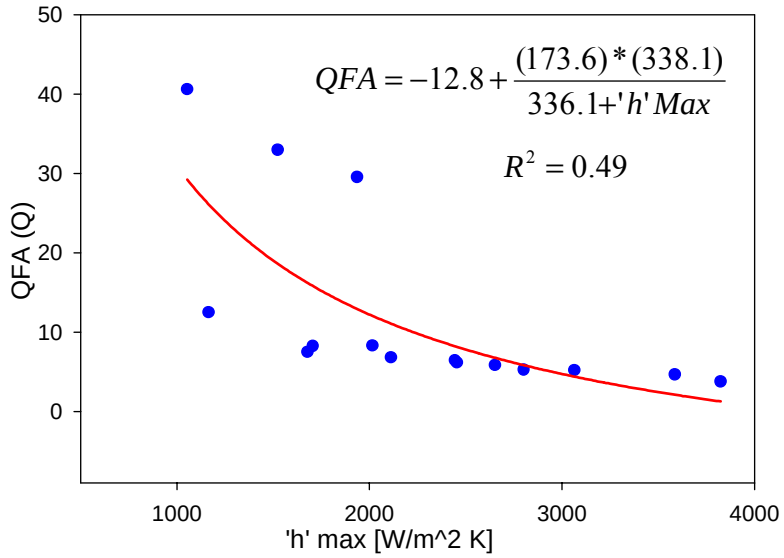


**Figure 9: Hyperbolic Regression of QFA as a Function of 'h' Max**

Figure 10 presents a second method of analyzing the data in Figure 9. The figure below presents the correlation between these two parameters in terms of a linear regression. The data at the bottom of the figure can be fit with a linear regression curve with a high correlation coefficient. The line of best fit is not representative of the data as a whole because the labeled data points to the left are not included in the linear relationship.

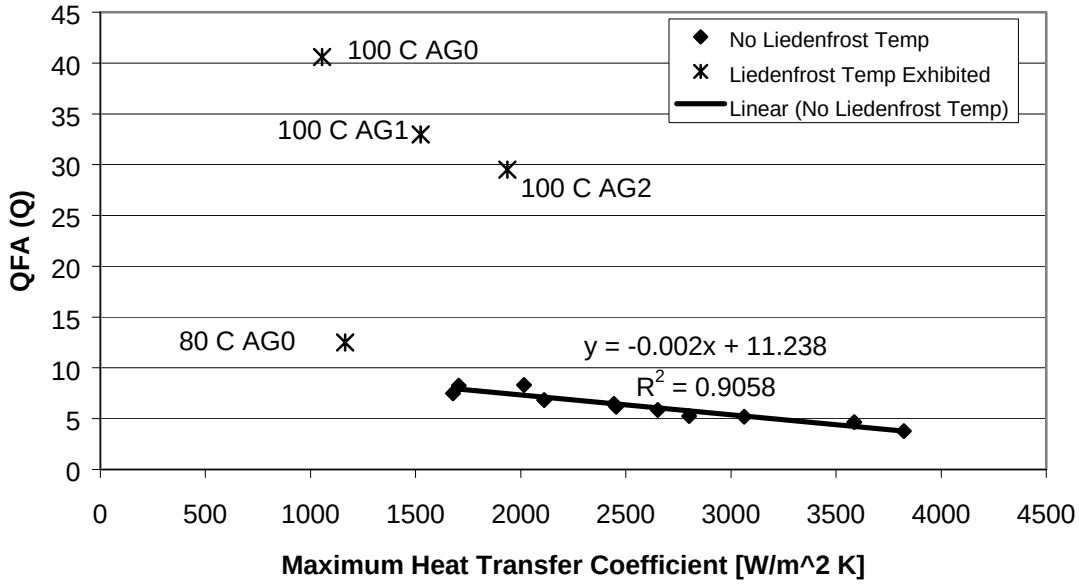


**Figure 10: Quench Factor As a Function of Maximum Heat Transfer Coefficient**

Upon further investigation, the eliminated data points were found to be the conditions with a Liedenfrost point present in their heat transfer coefficient curves. It appears that data with this point present cannot be compared to data without it. One explanation is that since the Liedenfrost point drives the temperature at which maximum heat transfer occurs to a lower temperature, the Q calculation in the Quench Factor Analysis is not summing the values at 'h' max, but rather at the temperature of the Liedenfrost point. As a result, these values are quite high and will not correlate well with the data collected from curves without a Liedenfrost point. Figure 11 illustrates the regions of interest on the heat transfer coefficient curve.

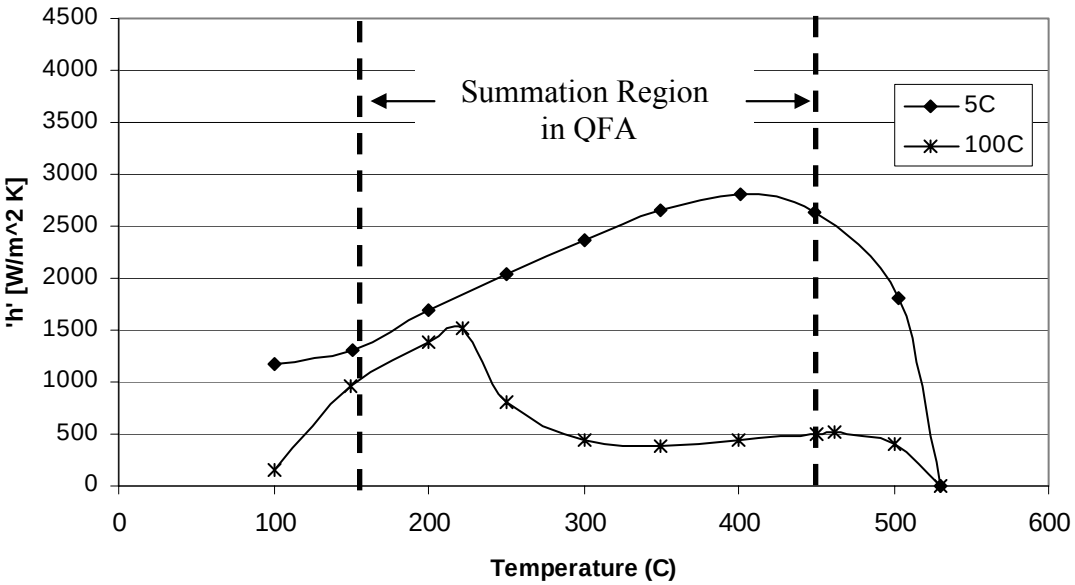


**Figure 11: Summation Region of Q as Seen on Heat Transfer Coefficient Curves**

The dashed lines represent the summation region in the QFA calculation [9]. Looking at the curve for 5°C, it is clear to see that the summation region is focused mainly on the location of maximum heat transfer, whereas at 100°C, the region is focused around the location of the Liedenfrost point. As a result, the majority of the summation values are coming from a region of very low heat transfer and not from the location of the

maximum heat transfer coefficient. In addition, if the stages of quenching are superimposed onto the curves above, it can be seen that the summation region at 5°C is mainly nucleate boiling, whereas at 100°C, the region encompasses film boiling and nucleate boiling. For these reasons, it is concluded that conditions with a Liedenfrost point cannot be directly compared to those without by means of QFA and 'h' relationship.

## Conclusions

Based on the experimental data presented above, it can be concluded that:

- An increase in agitation causes an increase in maximum heat transfer coefficient and a decrease in Quench Factor, Q.
- A decrease in bath temperature causes an increase in maximum heat transfer coefficient and a decrease in Quench Factor, Q.
- When a relationship between QFA and 'h' max is desired, conditions with a Liedenfrost point cannot be directly compared to those without due to the location of the summation region used in Quench Factor Analysis.

## References


1. ASM, *Quenching and Distortion Control*, ed. H.E. Boyer. 1998, Metals Park Ohio: ASM International.
2. Mackenzie, D.S. and G.E. Totten, *Aluminum Quenching Technology: A Review.* Materials Science Forum, 2000. **Vol. 331-337**: p. 589-594.
3. Hasson, J. *Quenchants: Yesterday, Today, and Tomorrow*. in *Proceedings of the First International Conference on Quenching and Control of Distortion*. 1992 September. Chicago, Illinois.
4. ASM, ed. *Aluminum and Aluminum Alloys: ASM Specialty Handbook*., ed. J.R. Davis. 1993, ASM International.
5. Mills, A.F., *Heat Transfer*. 2nd Ed ed. 1999, Upper Saddle River, NJ,: Prentice Hall.
6. Bates, C.E., G.E. Totten, and N.A. Clinton, *Handbook of Quenchants and Quenching Technology*. 1993, Materials Park, Ohio: ASM International.
7. Brimacombe, J.K., S.M. Gupta, and E.B. Hawbolt. *Determination of Quench Heat-Transfer Coefficients Using Inverse Methods*. in *Proceedings From the First*

*International Conference on Quenching and Control of Distortion*. 1992 September. Chicago, Illinois.
8. University, P., *Thermophysical Properties of Matter*. Specific Heat: Metallic Elements and Alloys, ed. Y.S. Touloukian. Vol. 4. 1970, New York: Purdue Research Foundation - Thermophysical Properties Research Center (TPRC).
9. Bates, C.E., L.M. Jarvis, and G.E. Totten, *Use of Quenching Factor for Predicting the Properties of Polymer Quenching Media.* Metal Science and Heat Treatment, 1996. **Vol. 38**(No. 5-6): p. 248-251.
10. Bates, C.E., T. Landig, and G. Seitanikis, *Quench Factor Analysis: A powerful Tool Comes of Age.* Heat Treating, 1985(December): p. 13-17.
11. Bates, C.E. and G.E. Totten. *Application of Quench Factor Analysis to Predict Hardness Under Laboratory and Production Condition*. in *Proceedings of the First International Conference on Quenching and Control of Distortion*. 1992 September. Chicago, Illinois.
12. Bates, C.E., G.E. Totten, and L.M. Jarvis, eds. *Quench Factor Analysis: Polymer vs. Hot Water*., ed. I. Tenaxol. 1994: Milwaukee, Wisconsin.
13. Bates, C.E., G.E. Totten, and G.M. Webster, *Cooling Curve and Quench Factor Characterization of 2024 and 7075 Aluminum Bar Stock Quenched in Type 1 Polymer Quenchants.* Heat Transfer Research, 1998. **Vol. 29**(No. 1-3).
14. Bernardin, J.D. and I. Madawar, *Validation of the Quench Factor Technique in Predicting Hardness in Heat Treatable Aluminum Alloys.* International Journal of Heat and Mass Transfer, 1995. **Vol. 38**: p. 863-873.
15. Staley, J.T., *Effect of Quench Path on Properties of Aluminum Alloys.* JTS Alcoa Laboratories.: p. 396-407.
16. Staley, J.T., *Quench Factor Analysis of Aluminum Alloys*. 1987, The Institute of Metals: London, England. p. 923-934.
17. Bates, C.E., G.E. Totten, and G.M. Webster. *Aluminum Quenching with Polymer Quenchants: An Overview*. in *17th ASM Heat Treating Society Conference Proceedings Including the 1st International Induction Heat Treating Symposium*. 1997 September. Indianapolis, Indiana.
18. Maniruzzaman, M., J.C. Chaves, and R.D. Sisson. *CHTE quench probe system - a new quenchant characterization system*. in *5th International Conference on Frontiers of Design and Manufacturing*. 2002. Dalian, China.
19. Maniruzzaman, M. and J.R.D. Sisson. *Investigation of bubble nucleation site density during quenching heat treatment process using video imaging*. in *TMS Annual Meeting 2002*. 2002. Seattle, WA.
20. Sisson, R.D., J.C. Chaves, and M. Maniruzzaman. *The Effect of Surface Finish on the Quenching Behavior of 4140 Steel in Mineral Oils*. in *Proceedings of the 21st Heat Treating Society Conference*. 2001. ndianapolis, Indiana.
21. Fontecchio, M. *Effect of Bath Temperature and Agitation Rate on the Quench Severity of 6061 Aluminum Quenched in Distilled Water*. in *13th Annual International Federation*

*for Heat Treatment & Surface Engineering (IFHTSE) Congress*. 2002. Columbus, Ohio.
22. Chaves, J.C., M. Maniruzzaman, and J.R.D. Sisson. *A New Quench Characterization System for Steels*. in *Proceedings of the 21st Heat Treating Society Conference*. 2001. Indianapolis, Indiana.

23. Maniruzzaman, M. and R.D. Sisson. *Bubble Dynamics During Quenching of Steel*. in *ASM Heat Treating Society*. 2001. Indianapolis, Indiana.
24. Chaves, J.C., *The Effect of Surface Finish Conditions and High Temperature Oxidation on Quenching Performance of 4140 Steel in Mineral Oil*. 2001 November 20, Worcester Polytechnic Institute.
25. Han, S.W., G.E. Totten, and S.G. Yun. *Continuously Variable Agitation in Quench System Design*. in *Proceedings From the First International Conference on Quenching and Control of Distortion*. 1992 September. Chicago, Illinois.

## APPENDIX A: Polyalkylene Glycol (PAG) Quenching

There are several commercial polymers quenchants that are readily accepted and used today such as Polyvinyl Alcohol, Polyvinylpyrrolidone, Polyacrylates, and Polyalkylene Glycol (PAG). Of these, PAG's are most common and will be considered extensively in this chapter [1].

The molecular formula for PAG is as follows:

$$HO - (CH_2 - CH_2 - O)_n - (CH_2 - \underset{\displaystyle CH_3}{\underset{|}{CH}} - O)_n - H$$

High molecular weight PAG is completely soluble in water at room temperature and therefore has been used extensively in the quenching of hot metal. PAG also exhibits a unique property in which it has inverse solubility as temperature increases in the water. As the temperature rises, the PAG precipitates out of the solution and deposits on the surface of the part. The deposited layer serves as an insulator, which, in turn, governs the rate of heat extraction from the quenched part. This layer also causes complete wetting of the surface and therefore does not prolong the vapor blanket stage. As a result, a more uniform quench is experienced and the risk of distortion and cracking is minimized. As the temperature of the part decreased, the polymer dissolves back into the aqueous solution and maintains the concentration of the quenchant bath [2].

The three main factors that govern the rate of heat transfer with the use of PAG quenchants include:

1. Quenchant concentration
2. Quenchant temperature
3. Quenchant agitation

This relationship between polymer concentration and quench rate can be attributed to the insulating layer that is deposited on the surface of the part as the temperature increases in the bath [1]. If there exists is a greater concentration of PAG in the bath, then the deposited insulating layer will be thicker. As a result, the rate of heat transfer will be controlled to a greater extent and slowed considerably. On the other hand, if the concentration is low, the insulating layer will be thin and the cooling rates achieved will approach those of plain water.

A similar relationship between bath temperature and quench rate is also well understood. As was the case with water, the cooling rates decrease as the temperature of the bath increases. This is due, primarily, to the thermal gradients that exist between the hot part and the bath temperature. If the gradient is high, then the cooling rate and the rate of heat transfer will also be high.

Finally, the relationship between agitation and cooling rate is understood by knowing that as the degree of agitation increases, so does the cooling rate. The use of some degree of agitation in PAG systems is almost essential. Agitation will allow adequate amounts of the polymer to come in contact with the hot surface and create its insulating layer as well as provide uniform heat transfer from the hot surface to the cooler liquid. These two factors will create a faster quench, uniform hardness and better mechanical properties [2].

In addition to the benefits that polymers exhibit in quenching, several concerns exist in the minds of some consumers [1]. Some are concerned with the potential contamination of water vapor from the quenchant in carburizing atmospheres, its corrosion protection, and its overall quenching performance. One study compared the

performance of PAG to oil in the quenching of an 8620 steel. The same procedure was carried out and physical properties were measured to compare the effectiveness of both mediums. Table 1 shows the collected data after the quench.

| Property | Oil Quench | Polymer Quench |
|---|---|---|
| % Martensite (at surface) | 56 | 86 |
| % Carbon (at surface) | 1.6 - 1.8 | 1.6 - 1.8 |
| Hardness at surface (Rc) | 59 – 64 | 63 - 64 |
| Hardness at Core (Rc) | 45 | 44 - 45 |

**Table A.1:** Comparison of AISI Carburized 8620 Metallurgical Properties of and Oil and Polymer Quench

The use of the PAG quench outperformed the oil quench in two of the four categories. The percentage of martensite on the surface was much greater with PAG than with oil, which indicates that the cooling rate was higher allowing more austenite to convert during the quench. In addition, the range of hardness values was smaller, indicating that the uniformity of the hardness was greater. Therefore, it can be said that the PAG quenchant outperformed the quenching oil considerable [1]. In addition, it is important to note that no corrosion was encountered on the quenched parts and no water contamination was experienced in the bath. As a result, many of the concerns of consumers were eliminated by this study.

In addition, this study showed that PAG was also more cost efficient on an annual basis, costing 28% less than the oil [1].

Although PAG shows promise in its quenching ability, several precautions must be taken to maintain its performance over time. The concentration of the bath must be

maintained to ± 1.0 % [3]. If the concentration varies considerably, the rates of heat transfer will change from quench to quench. Furthermore, the bath temperature should not rise more than 10°C to ensure that thermal gradients do not vary as different parts are quenched [2]. In terms of agitation, the system must be on prior to the quench to minimize the potential for water contamination of the furnace atmosphere.

In addition to these factors, the degradation of the polymer itself is also very important. The operator must ensure that the polymer is not degrading below an unacceptable level. As the polymer degrades and the molecular weight decreases over time, the quench rates will increase and the insulting layer that controls the rate of heat transfer is effectively lost [3].

**Figure A.1:** Comparison of Old and New Polymer Cooling Curves

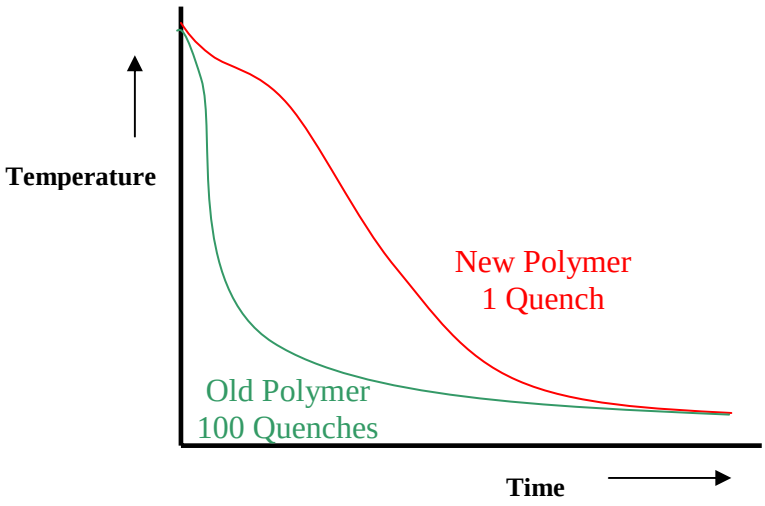


Several tests can be done to determine the degree of degradation of the polymer. Viscosity of the solution, which depends directly on the molecular weight of the polymer, can be measured and compared to a control to ensure that the viscosity level is not dropping over time. Also, a refractive index measurement can be taken. This test is not

sensitive to molecular weight, but is sensitive to polymer concentration, polymer degradation and impurities in the bath. It is a rapid test, so it is preferred among several industrial plants [3]. These tests will allow the user to monitor the degradation level of the polymer in the bath over time.

## TAGUCHI EXPERIMENTAL APPROACH

Dr. Genechi Taguchi is a Japanese scientist who spent most of his life researching ways to improve the quality of manufactured parts [4]. His approach stemmed from the work conducted by Sir R.A. Fisher who tried to determine the optimal growing conditions to produce the best crops. Fisher was able to lay out the possible combinations that could be used in a matrix, which allowed each factor an equal number of test conditions. Taguchi realized that to carry out all possible combinations would take far too long; so much work was done to statistically eliminate test conditions and reduce the total number of experiments to conduct. The table below shows several testing criteria including the number of factors and the number of levels associated with each factor. It also shows the total number of possible combinations that are present and the corresponding number of experiments proposed by Taguchi.

**Table A.2** Various Experimental Situations and Corresponding Taguchi Experiment Size

| Experimental Situation | Maximum Possible Conditions | Number of Taguchi Experiments |
|---|---|---|
| 3 two-level factors | 8 | 4 |
| 7 two-level factors | 128 | 8 |
| 11 two-level factors | 2024 | 12 |
| 15 two-level factors | 32768 | 16 |
| 4 three-level factors | 81 | 9 |
| 7 three-level factors | 2187 | 18 |

It is clear to see from the table above that the number of total experiments is reduced considerably by using the Taguchi approach. The highlighted row above indicates the experimental situation of interest. A situation with 4 three-level factors is termed an $L^9$ array. Although the maximum number of factors is equal to 4, an $L^9$ array can be used in the following three ways [4]:

1. 2 three level factors
2. 3 three level factors
3. 4 three level factors

In this research, 3 three level factors will be considered, so an $L^9$ array fits the experimental design criteria. An $L^9$ array is shows below with the corresponding levels of each factor placed in the matrix to dictate the testing conditions.

**Table A.3:** $L^9$ Orthogonal Array for Experimental Testing

| Condition Number | A | B | C | D |
|---|---|---|---|---|
| | Level | | | |
| 1 | 1 | 1 | 1 | 1 |
| 2 | 1 | 2 | 2 | 2 |
| 3 | 1 | 3 | 3 | 3 |
| 4 | 2 | 1 | 2 | 3 |
| 5 | 2 | 2 | 3 | 1 |
| 6 | 2 | 3 | 1 | 2 |
| 7 | 3 | 1 | 3 | 2 |
| 8 | 3 | 2 | 1 | 3 |
| 9 | 3 | 3 | 2 | 1 |

Columns A, B, and C will be utilized while Column D will not since there are only 3 factors to be considered in the experiment of interest.

Once the recommended experiments are carried out, a statistical analysis called Analysis of Variance (ANOVA) is conducted to determine the optimal condition for running a particular process as well as the contribution of each factor in the experiment.

## ANOVA CALCULATIONS

**Table A.4:** $L^9$ Array with Results Column

| Condition Number | A | B | C | Ave Result |
|---|---|---|---|---|
| | | Level | | |
| 1 | 1 | 1 | 1 | R1 |
| 2 | 1 | 2 | 2 | R2 |
| 3 | 1 | 3 | 3 | R3 |
| 4 | 2 | 1 | 2 | R4 |
| 5 | 2 | 2 | 3 | R5 |
| 6 | 2 | 3 | 1 | R6 |
| 7 | 3 | 1 | 3 | R7 |
| 8 | 3 | 2 | 1 | R8 |
| 9 | 3 | 3 | 2 | R9 |

The table above is the L9 array with the results column shown to its right. This column contains the average of several trials at a given condition. The results column can contain a variety of information. For the research contained in this thesis, the results column can be filled with QFA, maximum cooling rate, or maximum heat transfer coefficients. For the purpose of this analysis, the values will be shown as R1 to R9.

Once tabulated, the Analysis of Variance (ANOVA) can begin. The analysis starts with a calculation of the standard deviation of the results carried out by the equation below:

$$S_T = \sum_{i=1}^{N} (R_i - \overline{R})^2$$

To determine the variation caused by an individual factor (A, B, or C), a 'factor sum of squares' calculation is performed. The equation below shows this calculation for factor A.

$$S_A = \frac{A_1^2}{N_{A1}} + \frac{A_2^2}{N_{A2}} + \frac{A_3^2}{N_{A3}} - \left( \frac{T^2}{N} \right)$$

$A_1$ = The sum of the results for trials containing factor A at level 1
$A_2$ = The sum of the results for trials containing factor A at level 2
$A_3$ = The sum of the results for trials containing factor A at level 3
$N_{A1}$ = Total number of experiments containing factor A at level 1
$N_{A2}$ = Total number of experiments containing factor A at level 2
$N_{A3}$ = Total number of experiments containing factor A at level 3
T = Total of all results values
N = Total number of results
$T^2/N$ = Correction Factor

The two previous calculations were the basic equations needed for ANOVA. The following equations are also necessary:

$$Mean Squares (Variance): V_A = \frac{S_A}{f_A}$$

$f_A$ = Degrees of Freedom of Factor A: Equal to the number of levels to factor A -1

$$F - Ratio: F_A = \frac{V_A}{V_e}$$

$V_e$ = Variance for error term
(Calculated by dividing the error sum of squares by error degrees of freedom)

$$Pure Sum of Squares : S_A' = S_A - (V_e * f_A)$$

$$Percent Influence : P_A = \frac{S_A'}{S_T}$$

With these calculations, a table can be created to see the overall effect of each of the factors and their contribution to the total experiment.

**Table A.5:** ANOVA Table

| Column#/ Factor | DOF (f) | Sum of Squares (S) | Variance (V) | F-Ratio (F) | Pure Sum (S') | Percent P(%) |
|---|---|---|---|---|---|---|
| **Factor A** | 2 | SA | VA | FA | S'A | PA |
| **Factor B** | 2 | SB | VB | FB | S'B | PB |
| **Factor C** | 2 | BC | VC | FC | S'C | PC |
| **Error** | 0 | | | | | 0 |
| **Total** | | | | | | 100% |

The summation of PA, PB, and PC must equal 100% since they all contribute to the experiment, so they all play a role in its outcome. If one or more of the percentages in less than 10% of the total value, it becomes 'pooled' and the calculations are carried out again without that particular factor's influence.

A software called Qualitek-4: Automatic Design and Analysis of Taguchi Experiments (Q4) will be utilized for this analysis. This piece of software will also calculate the optimal conditions for the desired output of the process. For example, say a low value of QFA is desired, we can select, 'Smaller is Better' on the software and it will

determine the conditions necessary to create the smallest QFA as well as the predicted value given those particular conditions. A similar process known as "Bigger is Better' can be carried out for an analysis for maximum cooling rate or maximum heat transfer coefficient.

Although it is important to understand how to calculate all ANOVA variables, For the experiments conducted in this thesis, Q4 will be used for all calculations.

### 3.4.2 Polymer Testing

In the case of the polymer solution, Houghton Aqua Quench 260 was selected. For polymers, three variables were determined to be, bath temperature, agitation level and polymer concentration. Within these variables, there exists three levels in each for a total of 81 different combinations or conditions to test. At 5 runs per condition, it would have been necessary to conduct 405 quenches to fully analyze the data. As a result, the Taguchi Method for experimental design will be instituted to statistically eliminate the total number of quenches. In doing so, we will be able to determine interactions between parameters. The test matrix below illustrates an $L_9$ ($3^4$) layout for testing [5].

**Table A.6:** Taguchi Design of Experimentation for Polymer Quenching

| Factor | Level 1 | Level 2 | Level 3 |
|---|---|---|---|
| **A:** Polymer Concentration, % | 10 | 20 | 30 |
| **B:** Bath Temperature, degree C | 25 | 33 | 40 |
| **C:** Agitation Rate, rpm | 880 | 1390 | 1850 |

**Table A.7:** Taguchi Test Matrix for Polymer Quenching

$L_9 (3^4)$

| Condition Number | A % | B deg C | C Level | D |
|---|---|---|---|---|
| 1 | 10 | 25 | 880 | |
| 2 | 10 | 33 | 1390 | |
| 3 | 10 | 40 | 1850 | |
| 4 | 20 | 25 | 1390 | |
| 5 | 20 | 33 | 1850 | |
| 6 | 20 | 40 | 880 | |
| 7 | 30 | 25 | 1850 | |
| 8 | 30 | 33 | 880 | |
| 9 | 30 | 40 | 1390 | |

The variables above are classified as letters A-D for simplicity. The breakdown can be seen in Table A.2 above. Looking at Table A.3, it can be see that there are only 9 conditions to be tested and as a result only 45 quenches need to be done. The temperature range to be analyzed is small, while the concentration and agitation levels vary considerably. The actual values can be seen in the table above.

## REFERENCES


1. Bautista, B., D. Diaz, and H. Garcia. *Conversion and Use of Polymer Quenchants in Integral Quench Furnace Applications*. in *Proceedings of the First International Conference on Quenching and Control of Distortion*. 1992 September. Chicago, Illinois.

2. Mackenzie, D.S. and G.E. Totten, *Aluminum Quenching Technology: A Review*. Materials Science Forum, 2000. Vol. 331-337: p. 589-594.

3. Cordoba, E.V. *Eleven Years Quenching with PAG (Polyalkylene Glycol)*. in *Proceedings of the First International Conference on Quenching and Control of Distortion*. 1992 September. Chicago, Illinois.
4. Roy, R.K., *Design of Experiments Using the Taguchi Approach: 16 Steps to Product and Process Improvement*. 2001, New York, New York: John Wiley and Sons Inc.

5. Roy, R., *A Primer on the Taguchi Method*, ed. V.N. Reinhold. 1990: Competitive Manufacturing Series.

# 6.0 RECOMMENDATIONS AND FUTURE WORK

After completing the research contained within this thesis, it is possible to extend this area of research by means of using different alloys and quenching mediums. Having worked extensively with the current CHTE probe quenching system, several problems exist and can be changed to improve the data acquisition and ease of use.

## 6.1 Modifications to CHTE Probe-Quench System

The CHTE probe quenching system should be modified such that each component is electrically isolated from every other component. The steel table that is currently used should be eliminated and replaced with a frame which would increase the access to each component and eliminate grounding issues during the data collection. By isolating the agitation unit, quench tank and furnace, the level of electrical noise collected by the thermocouple will also be reduced. As a result, smoother data will be collected during the quench.

In addition to the overall layout, it should be noted that an ungrounded K-type thermocouple should be used with this system since it picks up a smaller amount of outside noise and does not get 'shorted' by contact with external metal surfaces. Furthermore, electrochemical noise occurring between the thermocouple sheath and probe center will not be transmitted through the thermocouple and seen in the collected data.

The constant temperature quench tank is also an item of concern. The Blue M tank used is adequate for quenching and is very convenient in heating the quench bath, but is does not allow the user the ability to videotape the quench as it is taking place. Additional experiments must be conducted in a plexyglass tank for videotaping purposes.

For this reason, it is recommended that this tank be changed. Also, as seen in the results presented in the paper entitled "The Effect of Bath Temperature and Agitation Rate on the Quench Severity of 6061 Aluminum in Distilled Water", as the level of agitation is increased, a high level of scatter in the data is observed. The agitation mechanism must be improved to provide better fluid flow towards the part being quenched and thus reduce the high degree of scatter.

To alleviate the heating and agitating problems associated with the quench tank, it is suggested that the current tank be replaced with one constructed out of plexyglass. By doing so, the videotaping issue is solved and experiments can be taped as they are conducted. Furthermore, an immersion heater and pump must be purchased in order to created a heated and agitated quench bath. The only issue with this tank is the risk of meting the plexyglass with the immersion heater. So, the tank must be designed such that the immersion heater does not make contact with the walls of the tank.

Once these changed are made, it is recommended that the experiments conducted in this thesis be redone. By collecting data with the current system and the proposed system, it will be possible to make comparisons on the effect of agitation design as well as show the importance of eliminating noise from data collection. In addition to 6061 aluminum, other heat-treatable alloys in the 2000, 6000 and 7000 series can be quenched and analyzed via Quench Factor Analysis and Cooling Rate Data

## 6.2 Polymer Quenchants

As stated in this thesis, many heat treaters are turning to aqueous polymer solutions as their quenching medium since it offers good control of cooling rates and allows cooling rates between water and oil quenching to be achieved [24].

Aqua Quench 251, 260 and 3600 have been acquired from Houghton International to perform experiments to determine the effect of bath temperature, agitation rate, and polymer concentration on quench severity. To determine the effect of these variables, it is suggested that a Taguchi Design of Experimentation be utilized. A simple $L_9$ array can be used which allows a maximum of 4 variables with 3 levels in each. In this case, there are only 3 variables with 3 levels, but $L_9$ can still be used. By using a Taguchi Approach, a fewer number of experiments can be conducted while still collecting adequate data for statistical analysis.

Once the data is collected, Analysis of Variance (ANOVA) should be performed to determine which variables are most important when conducting a polymer quench. The groundwork and test matrix has already been laid out and can be seen in Appendix A. Within this appendix, a literature review of polymer quenching has been done as well as the layout for an $L_9$ Taguchi Experiment. In addition, the ANOVA calculations are presented and can simply be followed when these experiments are conducted.

The experiments should be conducted for all three types of Houghton Aqua Quench since the material is now available.

# 5.0 CONCLUSIONS

The following conclusions were drawn on the effect of bath temperature and agitation rate on the quench severity of 6061 aluminum probes in distilled water. These three conclusions were drawn through an analysis of Cooling Rate data and Quench Factor, Q.

1. An increase in agitation and a decrease in bath temperature causes an increase in cooling rate and a decrease in Quench Factor, Q. This variation in quenching parameters allows for a high temperature gradient to exist between the part and quenching medium as well as fresh bath water to be circulated to the quenched part. As a result, the quench rate increases and Q decreases indicating a more sever quench has occured.
2. The standard deviation and range of the cooling rates at all temperatures increases with agitation. For this reason, design of the agitation system is critical in providing continuous fluid flow to the part being quenched. If the fluid is not circulated properly, the repeatability from experiment to experiment will not be consistent.
3. The Quench Factor, Q, is an excellent parameter for characterizing the quenching system. The value, Q, directly changes as a function of both the bath temperature and level of agitation. Therefore, this variation proves that as the quench conditions change, Q is an acceptable parameter for quantifying the quench in terms of quenching medium and alloy used.

Similarly, conclusions were drawn on the effect of these parameters as determined through Quench Factor Analysis and heat transfer coefficient calculations.

1. An increase in agitation and a decrease in bath temperature causes an increase in maximum heat transfer coefficient and a decrease in Quench Factor, Q. Since 'h' is directly calculated from an experimental value of dT/dt, heat transfer coefficients should follow similar trends as those for cooling rate data. For this reason, they both react similarly as the quenching parameters are changed.
2. When a relationship between QFA and 'h' max is desired, conditions with a Liedenfrost point cannot be directly compared to those without due to the location of the summation region used in Quench Factor Analysis. The location of interest in this calculation focuses on the region of nucleate boiling and the location of maximum heat transfer for curves without a Leidenfrost temperature. When a curve possesses a Liedenfrost point, the summation region is focused mainly on a film boiling mechanism and then on nucleate boiling. For this reason, these two types of curves cannot be directly compared via QFA and 'h'.

## APPENDIX B: COOLING RATE PROGRAM

```
;**** Computation of Derivatives ****

;This transform takes an t,T data set with increasing
;ordered t values and computes the first and second
;derivatives.

;      ********** Input Variables **********

cx=3          ;t data column number
cy=4          ;T data column number

;      ************ RESULTS ************
;The results are placed into a block of 3 columns
;starting at column cr.  Columns
;cr to cr+2 contain the first two derivatives.
;Column cr+3 is for working variables.

cr=5          ;1st column of results block

;      ************ PROGRAM ************
cr1=cr
cr2=cr+1
cr3=cr+20       ;working column
n=size(col(cx))
cell(cr3,1)=cx
cell(cr3,2)=cy
cell(cr3,3)=cr

;compute first derivative for 3 to n-2 rows

nm1=n-1
nm2=n-2
cell(cr3,4)=cell(cx,2)-cell(cx,1)          ;dt1
cell(cr3,5)=(cell(cy,2)-cell(cy,1))
  /cell(cr3,4)                    ;dT1
;cell(cr1,1)=cell(cr3,5)
;cell(cr1,2)=cell(cr3,5)

dt2=-12*cell(cr3,4)           ;dt2

for i=3 to nm2 do
  dT2=(cell(cy,i-2)-8*cell(cy,i-1)+8*cell(cy,i+1)-cell(cy,i+2))/dt2    ;dT2
  cell(cr1,i)=dT2
end for
```

```
;cell(cr1,nm1)=(cell(cy,n)-cell(cy,1))/cell(cr3,4)*6
;cell(cr1,n)=cell(cr1,nm1)

;compute second derivative for 5 to n-4 rows

nm4=n-4
;cell(cr3,6)=(cell(cr1,2)-cell(cr1,1))
;  /cell(cr3,4)*6                    ;ddT1
;cell(cr2,1)=cell(cr3,6)
;cell(cr2,2)=cell(cr3,6)

for i2=5 to nm4 do
  ddT2=(cell(cr1,i2-2)-8*cell(cr1,i2-1)+8*cell(cr1,i2+1)-cell(cr1,i2+2))/dt2    ;ddT2
  cell(cr2,i2)=ddT2
end for

;cell(cr2,nm1)=(cell(cr1,n)-cell(cr1,1))/cell(cr3,4)*6
;cell(cr2,n)=cell(cr2,nm1)
```